UDC 546.26-162: 541.13:549.21 doi: 10.33609/2708-129X.91.2.2025.55-90

CHIRAL, FLUORINE-CONTAINING PHARMACEUTICALS

Jianlin Han[1*], Alicja Wzorek,[2] Gagan Dhawan[3,4,*], Wei Zhang[5,*], Alexander E. Sorochinsky[6,*], Daniel Baecker[7*], Taizo Ono[8], Karel D. Klika[9], Vadim A. Soloshonok[10,11*]

[1] Jiangsu Co-Innovation Center of Efficient Processing and Utilization of Forest Resources, College of Chemical Engineering, Nanjing Forestry University, Nanjing 210037, China;
[2] Institute of Chemistry, Jan Kochanowski University in Kielce, Uniwersytecka 7, 25-406 Kielce, Poland
[3]School of Allied Medical Sciences, Delhi Skill and Entrepreneurship University, Dwarka, New Delhi-110077, India;
[4] Department of Biomedical Science, Acharya Narendra Dev College, University of Delhi, Kalkaji, New Delhi-110019, India;
[5] Department of Chemistry, University of Massachusetts Boston, Boston MA 02125, Unites States;
[6] V. P. Kukhar Institute of Bioorganic Chemistry and Petrochemistry, The National Academy of Sciences of Ukraine, Kyiv 02094, Ukraine;
[7] Department of Pharmaceutical and Medicinal Chemistry, Institute of Pharmacy, Freie Universität Berlin, Königin-Luise-Straße 2+4, 14195 Berlin, Germany;
[8] National Institute of Advanced Industrial Science and Technology (AIST), 2266-98, Anagahora, Shimoshidami, Moriyama-ku, Nagoya, 463-8560, Japan;
[9] Research and Development Center, Archer Daniels Midland, 1001 N Brush College Rd., Decatur, IL 62521, USA;
[10] Department of Organic Chemistry I, Faculty of Chemistry, University of the Basque Country UPV/EHU, Paseo Manuel Lardizábal 3, 20018 San Sebastián, Spain;
[11] IKERBASQUE, Basque Foundation for Science, María Díaz de Haro 3, Plaza Bizkaia, 48013 Bilbao, Spain
email: vadimsoloshonok@gmail.com

Fluorine is a key element in drug design due to its ability to enhance metabolic stability, binding affinity, and bioavailability. Fluorine's properties lead to more stable drugs with longer half-lives, reducing dosing frequency and improving patient compliance. Its small size and high electronegativity also improve binding affinity, resulting in more effective treatments with lower doses. For example, fluorine increases a compound's ability to cross cell membranes. This article highlights advancements in chiral, fluorine-containing pharmaceuticals introduced over the past five years, focusing on their synthesis, therapeutic benefits, mechanisms of action, and the impact of fluorine on efficacy and safety. Chiral molecules, essential in drug development, exist in two enantiomeric forms with distinct biological activities. Synthesizing chiral, fluorine-containing drugs involves techniques like asymmetric synthesis to produce pure enantiomers, resulting in drugs with increased potency, selectivity, and reduced side effects. Understanding their mechanisms of action provides valuable insights into efficacy and safety. Reviewing recently FDA-approved chiral drugs offers insights into fluorine

chemistry in drug development and future therapeutic innovations. Recent FDA approvals highlight the significance of chiral, fluorine-containing drugs in various therapeutic areas, enabling targeted and effective treatments. Analyzing these approvals reveals trends shaping drug development's future. The article also addresses the need for more research into self-disproportionation of enantiomers (SDE) in chiral, fluorinated compounds and concerns about excessive fluorine levels. SDE can affect pharmaceutical product purity. Research into SDE in fluorinated compounds ensures drug quality. Additionally, fluorine's widespread use raises environmental and health concerns, necessitating studies on long-term effects and mitigation strategies.

Keywords: Fluorine, chirality, drug design, pharmaceuticals, self-disproportionation of enantiomers, bioactivity.

INTRODUCTION. Pharmaceuticals play a crucial role in modern medicine, significantly enhancing the quality of life for millions of people worldwide. They are essential for treating a wide range of diseases and conditions, from chronic illnesses to acute infections, and have revolutionized healthcare by providing effective and targeted therapies [1–5].

One of the key factors in drug design and development is chirality. The importance of chirality cannot be overstated as the spatial arrangement of atoms in a molecule can drastically affect a drug's efficacy and safety. Enantiomers can have different biological activities, often with one being therapeutically active while the other may be inactive or even harmful. Therefore, understanding and controlling chirality is vital for developing safe and effective pharmaceuticals. It comes as no surprise that over 70% of small-molecule drugs on the market today are chiral [6–11].

Fluorine has emerged as a critical element in drug design and development [12–14]. Its unique chemical properties, such as high electronegativity and small size, allow it to form strong bonds with carbon, enhancing the metabolic stability and binding affinity of drugs. Fluorine can also improve the bioavailability and pharmacokinetic profiles of pharmaceuticals rendering them more effective [15–19].

However, the synthesis of fluorine-containing compounds presents significant challenges, particularly in asymmetric synthesis. Achieving the desired chirality in fluorine-containing molecules requires sophisticated techniques and precise control over reaction conditions. The difficulties associated with these syntheses can complicate the drug development process and result in increased production costs [20–31].

Fluorine is also one of the most prominent self-disproportionation of enantiomers (SDE)-phoric groups [32–34] *i.e.*, the ability to express strongly the SDE phenomenon [35–37]. The SDE phenomenon leads to the enrichment of one enantiomer over the other during synthesis when fractionation is involved, which is crucial for producing enantiomerically pure drugs [38–40]. Thus, SDE tests are essential during the production of chiral, fluorine-containing drugs to ensure the desired enantiomeric purity and consequent therapeutic efficacy [41, 42].

Despite its benefits, fluorine-containing drugs have a dark side. Fluoride, a common form of fluorine, is a poison that can accumulate in the body over time. Chronic exposure to high levels of fluoride can lead to adverse health effects, including dental and skeletal fluorosis. Therefore, the use of fluorine in pharmaceuticals must be carefully managed to balance its therapeutic advantages against potential risks [43–49].

According to surveys published up to 2020 [12, 13, 50, 51], around 400 fluorine-containing pharmaceuticals have been approved by the FDA. Reviews from 2020–2024 profiled 50 new fluorine-containing, small-molecule pharmaceuticals [52–56]. Unsurprisingly, most of these drugs (~75%) are chiral and have been approved as specific enantiomers. For example, highly grossing drugs such as Asciminib (Scemblix™) **1** [57], Melflufen (Pepaxto™) **2** [58], and Krazati™ (Adagrasib) **3** [59] are all chiral (Fig. 1).

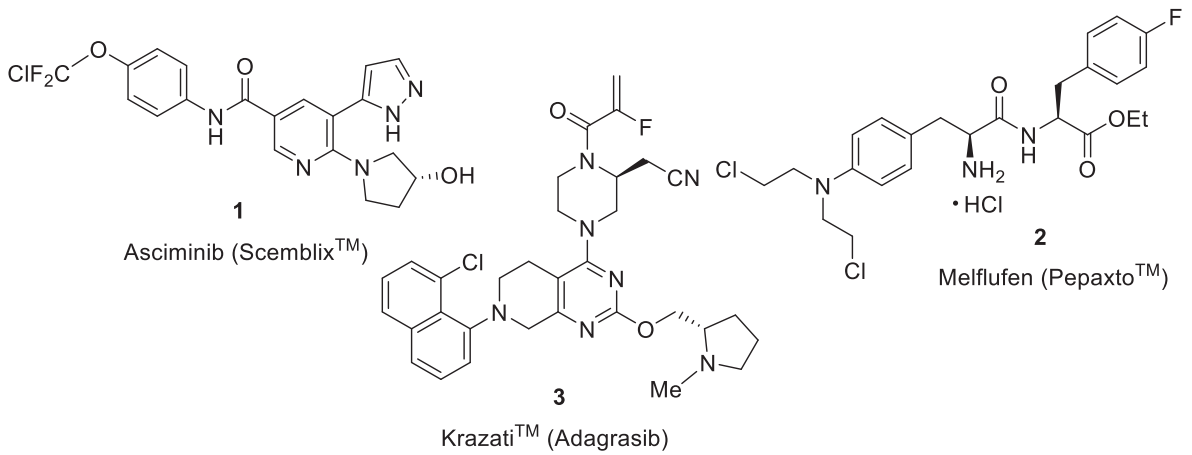

Figure 1. Examples of chiral, fluorine-containing compounds displaying stereogenic centers on residues of tailor-made amino acids or related amino alcohols and diamines.

However, the fluorine atom in these molecules is situated quite far from the stereogenic centers, consequently having minimal effects on their synthesis and chiral properties. Since most approved chiral compounds are based on amino acids or related amino alcohols and diamines, modern pharmaceuticals derived from tailor-made amino acids [60–65] and featuring fluorine constitute a unique and rapidly growing segment of the small-molecule pharmaceutical market [56, 66–68].

In this review, we profile compounds approved by the FDA during the period 2020–2024 that display fluorine or fluoroalkyl groups directly bonded to stereogenic centers. These structural features highlight the great impact fluorine can have on the asymmetric synthesis, chiro-optic, physical, and biological properties of these molecules. This group of compounds (Fig. 2) include: Fluoroestradiol F-18 (Cerianna™) **4**, a radioactive diagnostic agent used in positron emission tomography (PET) imaging to detect estrogen receptor-positive lesions in patients with recurrent or metastatic

breast cancer; Inqovi™ **5**, a combination of a nucleoside metabolic inhibitor and a cytidine deaminase inhibitor approved to treat adults with myelodysplastic syndromes including chronic myelomonocytic leukemia; Belzutifan (Welireg™) **6**, used to treat adults with von Hippel–Lindau (VHL) disease who require therapy for associated renal cell carcinoma, central nervous system hemangioblastomas, or pancreatic neuroendocrine tumors that do not need immediate surgery; Voranigo® (Vorasidenib) **7**, an isocitrate dehydrogenase-1 and isocitrate dehydrogenase-2 inhibitor prescribed to treat adults and pediatric patients aged 12 years or older with Grade 2 astrocytoma or oligodendroglioma following surgery that have a susceptible isocitrate dehydrogenase-1 or isocitrate dehydrogenase-2 mutation; Vivjoa™ (Oteseconazole) **8**, an antifungal medication used to reduce the risk of recurrent vulvovaginal candidiasis (RVVC) in females with a history of RVVC who are not potentially reproductive; Sunlenca™ (Lenacapavir) **9**, developed and administered in combination with other antiretroviral medicines to treat adults with HIV-1 infection who have received multiple HIV-1 medicines in the past and have the HIV-1 virus that is resistant to many HIV-1 medicines; Voydeya® (Danicopan) **10**, which inhibits complement Factor D that plays a key role in the immune system's alternative pathway and approved as an add-on therapy for adults with paroxysmal nocturnal hemoglobinuria who experience ongoing anemia due to extravascular hemolysis despite treatment with Ravulizumab (Ultomiris) or Eculizumab (Soliris); Jaypirca® (Pirtobrutinib) **11**, used to treat adults with relapsed or refractory mantle cell lymphoma, chronic lymphocytic leukemia, and small lymphocytic lymphoma who have received at least two prior lines of therapy, including a Bruton's tyrosine kinase inhibitor and a BCL-2 inhibitor; and finally, Itovebi® (Inavolisib) **12** prescribed in combination with Palbociclib and Fulvestrant to treat adults with hormone receptor-positive, human epidermal growth factor receptor 2-negative breast cancer that has an abnormal phosphatidylinositol-3-kinase catalytic subunit alpha gene, and has spread to nearby tissue or lymph nodes (locally advanced), or to other parts of the body (metastatic), and has returned after hormone (endocrine) therapy.

Fluoroestradiol F-18 (Cerianna™) **4**.

Estrogen receptors serve as crucial prognostic biomarkers enabling the visualization of tumor progression/regression or facilitating targeted hormone therapy. Molecules labeled with radioactive ^{18}F can accumulate in cancerous tissues expressing estrogen receptors, providing powerful contrast agents for diagnosis. These agents also allow for the assessment of estrogen receptor expression heterogeneity without the need for biopsy [69, 70]. Numerous ^{18}F-labeled radiopharmaceuticals have been documented in the literature for PET imaging [71–74]. Incorporating a small, highly electronegative fluorine atom as a hydrogen mimic can enhance pharmacokinetic and physicochemical properties, including binding affinity, metabolic stability, and bioavailability. The goal of developing high-affinity, estrogen receptor-targeted diagnostic agents capable of crossing the blood–brain barrier led to the synthesis of radioactive fluoroestradiols. These molecules exhibit high binding affinity for estrogen receptors and exceptional tissue permeability, including the blood–brain barrier [75, 76].

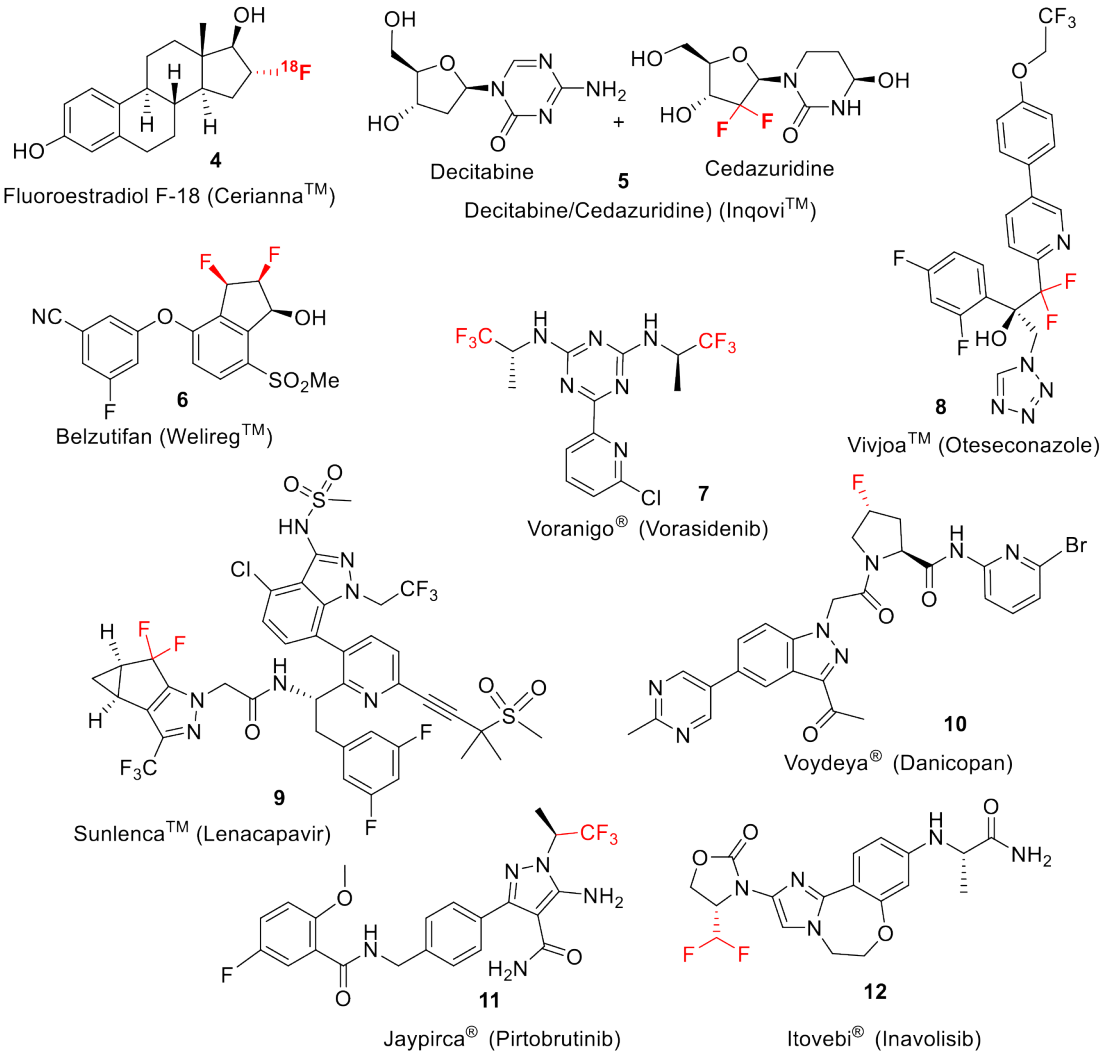

Figure 2. The structures of pharmaceuticals featuring fluorine or fluoroalkyl groups directly bonded to stereogenic centers.

Fluoroestradiol F-18 **4** (also known as [^{18}F]16α-fluoroestradiol) was developed by Zionexa USA and brought to market by Petnet Solutions, Zionexa USA's manufacturing arm and exclusive distributor in the USA. On May 20th, 2020, the FDA approved Fluoroestradiol F-18 **4** as a radioactive diagnostic agent for the non-invasive monitoring of estrogen receptor-positive lesions during PET scans in patients with recurrent or metastatic breast cancer. Fluoroestradiol F-18 **4** enables the detection of multiple tumor sites without causing patient discomfort. FDA's approval was primarily based on data from two published clinical trials [77, 78]. In these trials, all patients with recurrent or metastatic estrogen

receptor-positive breast cancer received Fluoroestradiol F-18 **4** prior to their PET scans and the results compared to tissue biopsy data.

Kiesewetter *et al.* pioneered synthetic procedures for preparing ^{18}F-labeled estrogens [78] and subsequently other research groups [79, 80] successfully synthesized fluoroestradiols. The ^{18}F radioisotope used in these syntheses is generated from ^{18}O-H_2O [79]. The synthesis of Fluoroestradiol F-18 **4** begins with compound **13** (Scheme 1), activated for nucleophilic substitution, which is reacted with $K^{18}F$ in anhydrous acetonitrile at 110 °C for 15 minutes to yield intermediate **14**. Following ^{18}F fluorination, the solution is then treated with 2 *N* HCl followed by neutralization with aqueous $NaHCO_3$. The crude product **4** is purified by semi-preparative HPLC using 50% aqueous ethanol as eluent [81]. The radiochemical yield can be as high as 43%.

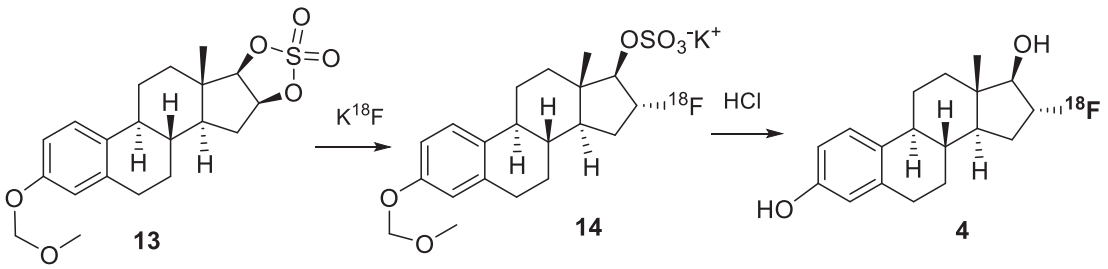

Scheme 1. The synthesis of Fluoroestradiol F-18 **4**.

*Decitabine/Cedazuridine (Inqovi™) **5**.*

Inqovi **5**, a fixed-dose combination of Decitabine **15** and Cedazuridine **17**, was developed by Astex Pharmaceuticals Inc., a subsidiary of Otsuka Pharmaceuticals. The FDA approved it on July 7th, 2020 for treating myelodysplastic syndromes and chronic myelomonocytic leukemia. Decitabine **15** (Fig. 3), a hypomethylating nucleoside metabolic inhibitor also known as a cytidine antimetabolite, incorporates itself into DNA after metabolism, inhibiting DNA methyltransferase in proliferating cancer cells. This leads to the reactivation of silenced tumor suppressor genes and apoptosis of cancerous cells, restoring normal cellular differentiation and proliferation [82–84].

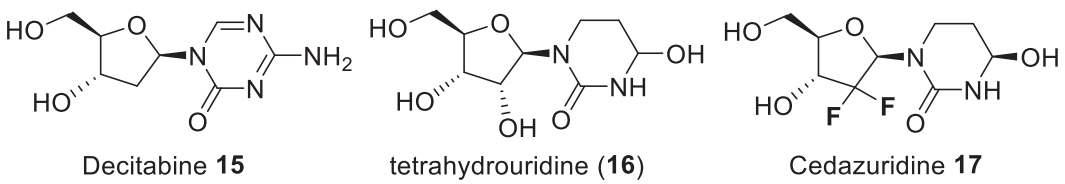

Figure 3. The structures of Decitabine **15**, tetrahydrouridine (**16**), and Cedazuridine **17**.

However, its oral bioavailability is limited due to first-pass metabolism by cytidine deaminase in the gut, kidney, and liver. To enhance oral bioavailability and reduce gastro-

intestinal toxicity associated with high-dose Decitabine **15**, the cytidine deaminase inhibitor tetrahydrouridine (**16**) is co-administered. This approach was patented by Otsuka Pharmaceutical Co. Ltd [85].

Cytidine and deoxycytidine are both substrates for CDA, demonstrating that the 2'-hydroxy group of cytidine does not play a specific role in binding [86, 87]. This was further confirmed by the co-crystal structure of mouse CDA with tetrahydrouridine (**16**), which revealed that only the 3'-OH and 5'-OH groups of the sugar form critical hydrogen bonds with specific amino acid residues in the active site [88]. Later studies showed that 2'-deoxytetrahydrouridine is more potent than tetrahydrouridine (**16**) [89]. To enhance acid stability and systemic exposure, Ferraris *et al*. developed 2'-fluorinated tetrahydrouridine derivatives, such as Cedazuridine **17**, as next-generation CDA inhibitors that prevent the breakdown and enhance the efficacy of Decitabine **15** in primates [90]. The acid-stable CDA inhibitor Cedazuridine **17** demonstrated improved stability in acidic environments and better oral bioavailability in rhesus monkeys compared to tetrahydrouridine (**16**) and its analogs. Co-administration with the CDA substrate Decitabine **15** resulted in increased plasma levels of Decitabine **15** in primates [90–93]. The orientation of the 4-hydroxyl group in **16** is crucial for CDA inhibition, explaining the difference in potency between its isomers. A similar binding mode and interaction with the active-site zinc atom were observed for fluorinated analogs. The FDA approved Cedazuridine **17** for combination with Decitabine **15**, marketed by Astex Pharmaceuticals Inc. under the name Inqovi™ **5**. This approval was based on phase III studies evaluating systemic exposure to Decitabine **15** from Inqovi™ **5** as well as its safety and efficacy [94].

The fluorinated analog of **16**, Cedazuridine **17**, is prepared using the procedures reported by the Sturla group [90] for the synthesis of 2′-deoxytetrahydrouridine. As illustrated in Scheme 2, gemcitabine **18** served as starting material. The first step is rhodium-catalyzed hydrogenation of **18** to form 2′-deoxy-2′,2′-difluorodihydrouridine (**19**). This is followed by reduction of **19** with $NaBH_4$ to give a mixture of difluorinated tetrahydrouridine **17** along with diastereomer **21** as well as the 4-deoxy byproduct **20**. Preparative HPLC is used to isolate enantiomerically pure Cedazuridine **17** in less than 30% yield.

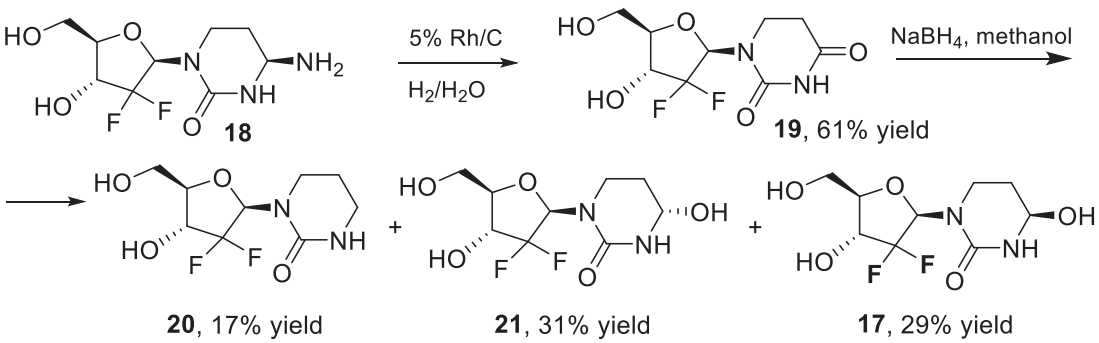

Scheme 2. The synthesis of Cedazuridine **17**.

Belzutifan (Welireg™) ***6***.

VHL disease is a rare genetic disorder that significantly increases the risk of developing multiple organ cancers [96, 97]. Renal cell carcinoma is often linked to the inactivation of the VHL protein, a crucial component of an E3 ubiquitin ligase complex responsible for protein degradation. The VHL protein primarily regulates hypoxia-inducible factors (HIF). HIF-2α, in particular, plays a vital role in renal cell carcinoma. Oxygen-dependent HIF prolyl-hydroxylase enzymes control the activity of HIF-2α by hydroxylating specific proline residues, creating a recognition site for VHL protein and targeting it for rapid proteasomal degradation. In patients with renal cell carcinoma, defective or absent VHL protein leads to the accumulation and transcriptional activation of HIF-2α [98, 99].

Several research groups have demonstrated that small molecules can allosterically inhibit the inner pocket of HIF-2α, reducing its protein–protein interaction with ARNT and thereby inhibiting transcriptional activity [100–103]. The first-generation HIF-2α inhibitor **22** (Fig. 4) developed through structure-guided studies showed clinical activity in advanced renal cell carcinoma patients [104]. However, its use was limited due to extensive phase 2 metabolism *via* glucuronide conjugation [105–107].

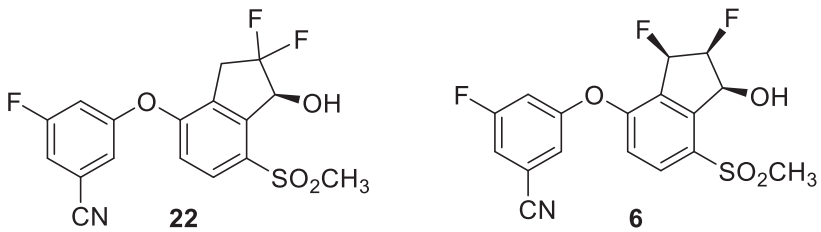

Figure 4. The structures of Belzutifan **6** and its structural precursor **22**.

Structural modification of compound **22** to Belzutifan **6**, achieved by altering its geminal difluoro group to a vicinal difluoro moiety, resulted in enhanced potency, reduced lipophilicity, and an improved ADME profile with decreased glucuronide conjugate formation. The FDA has approved Belzutifan (Welireg™) **6**, a hypoxia-inducible factor-2 alpha (HIF-2α) inhibitor developed by Merck, for treating cancers associated with VHL disease that do not require immediate surgery. As shown in Figure 4, Belzutifan **6** is a chiral compound with three adjacent stereogenic carbon atoms and three fluorine substitutions consisting of two C(sp^3)–F bonds and one C(sp^2)–F bond.

The synthesis of Belzutifan **6** (Scheme 3) begins with enantiomerically pure fluorinated alcohol **22** as starting material [108–110]. Compound **22** is converted into ester **23** in 87% yield by reaction with acetic anhydride in the presence of 4-(dimethylamino)pyridine and triethylamine. Ester **23** is then brominated by a radical reaction initiated by azodiisobutyronitrile with the use of *N*-bromosuccinimide at 80 °C for 3 hours giving rise to compound **24** in 65% yield. The treatment of **24** with $AgClO_4$ at 70 °C for 2 hours allows for the substitution of bromine by a hydroxy group furnishing alcohol **25** in low 23% yield but with the required configuration of the stereogenic

centers. Subsequently, stereoselective fluorination reaction of **25** with (diethylamino)sulfur trifluoride at −78 °C provides the vicinal difluoro compound **26** in 74% yield. Finally, the ester group in compound **26** is hydrolyzed by 0.5 *N* LiOH solution at 0 °C to afford Belzutifan **6**.

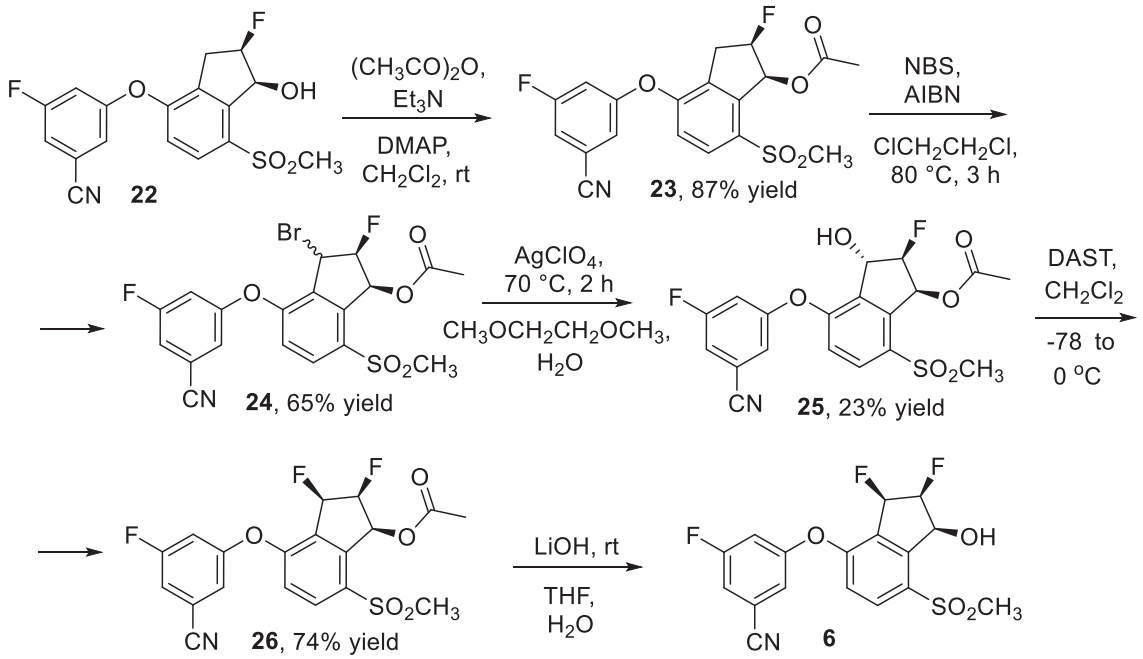

Scheme 3. The synthesis of Belzutifan **6**. Legend: AIBN, azodiisobutyronitrile; DAST, (diethylamino)sulfur trifluoride; DMAP, 4-(dimethylamino)pyridine; NBS, *N*-bromosuccinimide; THF, tetrahydrofuran.

Voranigo® (Vorasidenib) 7.

Gliomas are the most common malignant brain tumors in adults [111, 112]. A subset of these tumors harbor mutations in the genes encoding the metabolic enzymes IDH1 or IDH2 [112–118]. Gliomas with IDH1 or IDH2 mutations and an unbalanced translocation (1p/19q codeletion) are classified as oligodendrogliomas, while IDH-mutant gliomas without 1p/19q codeletion are defined as astrocytomas [119, 120]. These tumors are notorious for infiltrating normal brain tissue and, over time, progressing into more aggressive forms characterized by features such as neovascularization [121, 122]. Vorasidenib **7**, an orally administered, brain-penetrant drug with potential antineoplastic activity, acts as a dual inhibitor of the enzymes IDH1 and IDH2. By inhibiting the activity of mutant IDH1 and IDH2 enzymes in cancer cells, Vorasidenib **7** effectively slows the progression of brain tumors. In August 2024, Vorasidenib **7** received FDA approval for the treatment of Grade 2 astrocytoma or oligodendroglioma with susceptible IDH1 or IDH2 mutations [123].

Vorasidenib **7** demonstrates superior brain penetration and higher drug exposure compared to Enasidenib **28** (Fig. 5), a known trifluoromethyl-containing achiral drug [124–126]. In contrast to **28**, Vorasidenib **7** is a chiral

triazine derivative with two chiral centers both of *R* configuration. Structure–activity relationship studies revealed that introducing two trifluoromethyl groups led to excellent inhibition in the neurosphere TS603 cell assay using IDH1-R132H/IDH1-wild type cells with an IC_{50} of 0.6 nmol/L [124]. Replacing the trifluoromethyl groups with cyclopropyl groups (*i.e.*, compound **27**) resulted in a loss of inhibitory potency. While the racemate, **29**, displayed nanomolar potency, Vorasidenib **7** with *R*,*R* absolute configuration exhibited approximately ten-fold greater potency in cell assays [124]. Treatment with Vorasidenib **7** reduced the concentration of the oncometabolite 2-hydroxyglutarate which is linked to the reversal of gene expression and epigenetic alterations commonly observed in gliomas with IDH mutations [127–129].

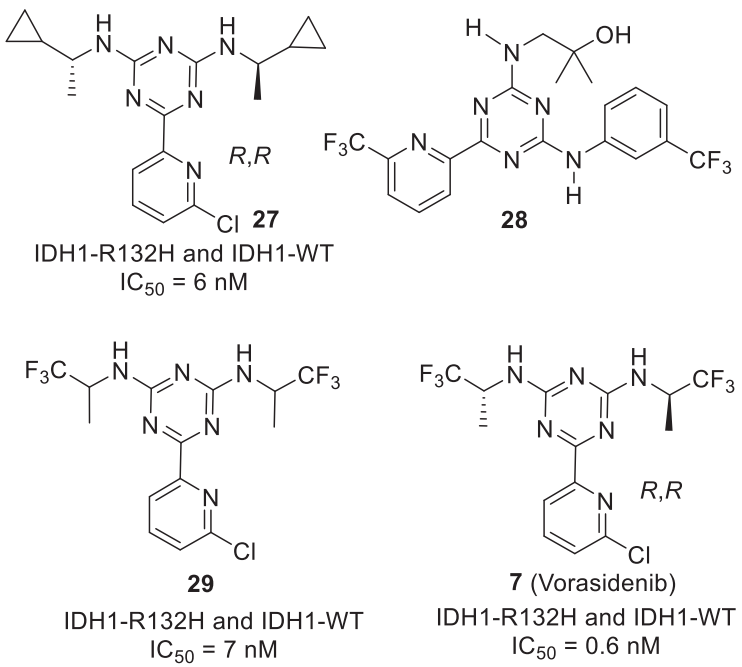

Figure 5. The structures of Vorasidenib **7** and its structural **27** and **28** and optical **29** analogs.

Vorasidenib **7** works by reducing the production of 2-hydroxyglutarate, which inhibits 2-hydroxyglutarate-mediated signaling. This action restores cellular differentiation and inhibits cellular proliferation in mIDH-mutant tumor cells. As a result, Vorasidenib **7** effectively treats certain forms of glioma by slowing tumor growth and delaying relapse [130–132].

The synthesis of Vorasidenib **7** (Scheme 4) [133] begins with the cyclization of bi-urea with methyl 6-chloropicolinate **30** using NaOEt as a base to furnish the 1,3,5-triazine intermediate **31**. Compound **31** is then treated with $POCl_3$ and PCl_5 to yield the 2,4-dichloro-1,3,5-triazine compound **32**. The reaction of **32** with (*R*)-1,1,1-trifluoropropan-2-amine HCl salt (**33**) in the presence of diisopropylethylamine [134] at 95–100 °C for 20 hours resulted in the formation of Vorasidenib **7** as an off-white solid after purification by crystallization. It

should be noted that the key chiral, fluorinated compound in this synthesis, (*R*)-1,1,1-trifluoropropan-2-amine [135–137] and related compounds featuring a trifluoromethyl group in the α position relative to the amino group, are readily available *via* biomimetic transamination of the corresponding keto compounds [138–141].

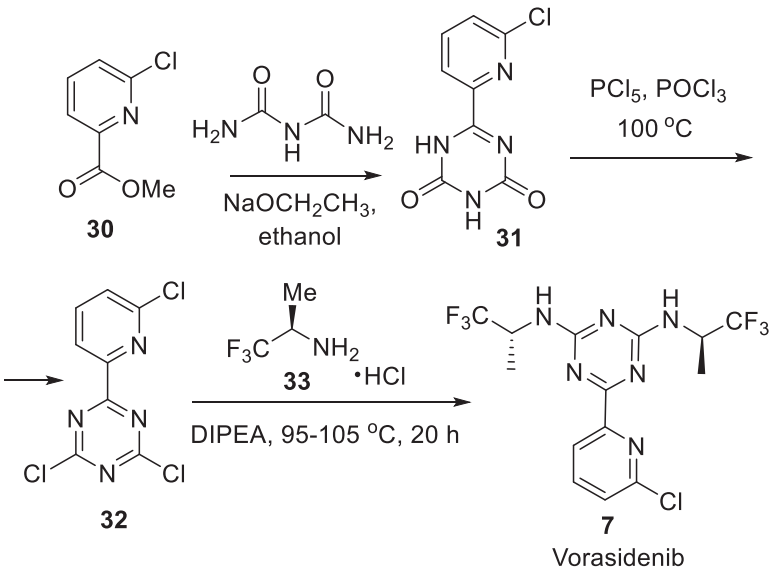

Scheme 4. The synthesis of Vorasidenib **7**. Legend: DIPEA, diisopropylethylamine.

Vivjoa™ (Oteseconazole) ***8****.*

Oteseconazole **8**, a potent oral antifungal agent developed by Mycovia Pharmaceuticals, belongs to the class of tetrazole antifungal agents [142]. It inhibits cytochrome P450 (CYP51) by disrupting the formation and integrity of the fungal cell membrane. In studies on *Candida albicans* cells, **8**'s binding strength to CYP51 was found to be similar to other azole antifungal agents, including Fluconazole, demonstrating tight binding inhibition. However, unlike other azole antibacterial agents, Oteseconazole **8** does not bind to human CYP51 or inhibit its activity [143, 144]. Research confirmed **8**'s effectiveness in treating initial episodes of VVC and highlighted its superior efficacy and safety in treating RVVC compared to the current standard care drug, Fluconazole, for VVC [145]. Oteseconazole **8** is a chiral compound featuring a difluoromethyl pyridine unit bonded to the stereogenic carbon, a tetrazole heterocyclic moiety, a difluorophenyl group at the chiral carbinol center, and a trifluoroethoxy group representing the third case of fluorination in this molecule. Structure–activity relationship studies by Viamet Pharmaceuticals Inc. revealed that replacing the trifluoroethyl ether with a chloro group in compound **34** (Fig. 6) led to a decrease in inhibitory activity against *Trichophyton rubrum* with the MIC increasing from < 0.001 to 0.004 μM. Additionally, Oteseconazole **8** demonstrated high selectivity for CYP3A4 *vs. T. rubrum* [146].

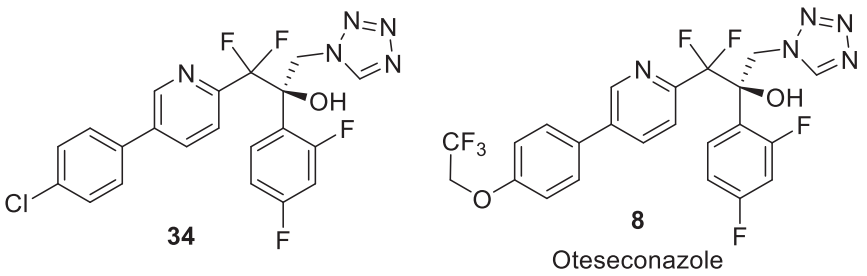

Figure 6. The structures of Oteseconazole **8** and its non-fluorinated analog **34**.

On April 26th, 2022 the FDA approved Vivjoa™ (Oteseconazole) **8** as an oral antifungal drug to reduce the incidence of recurrent RVVC in women with a history of RVVC who are not potentially reproductive. This makes it the first and only drug approved by the FDA specifically for RVVC [142].

The synthesis of Oteseconazole **8** is presented in Scheme 5. 2,5-Dibromopyridine is reacted with difluorobromoethyl acetate in the presence of Cu to yield the coupling product **35**. Compound **35** is next reacted with tetrazol-1-ethyl acetate to furnish the Claisen reaction product keto ester **36**. The next step involves the hydrolysis of the ester function followed by the decarboxylation of the carboxylic group to give ketone **37**. The *p*-ethoxy phenyl group is incorporated by Suzuki coupling of **37** with dioxaborolane **38**. Finally, compound **39** is reacted with the Grignard reagent derived from 2,4-difluorobromobenzene in the presence of chiral ligand (*R*)-BINOL to yield Oteseconazole **8** [147].

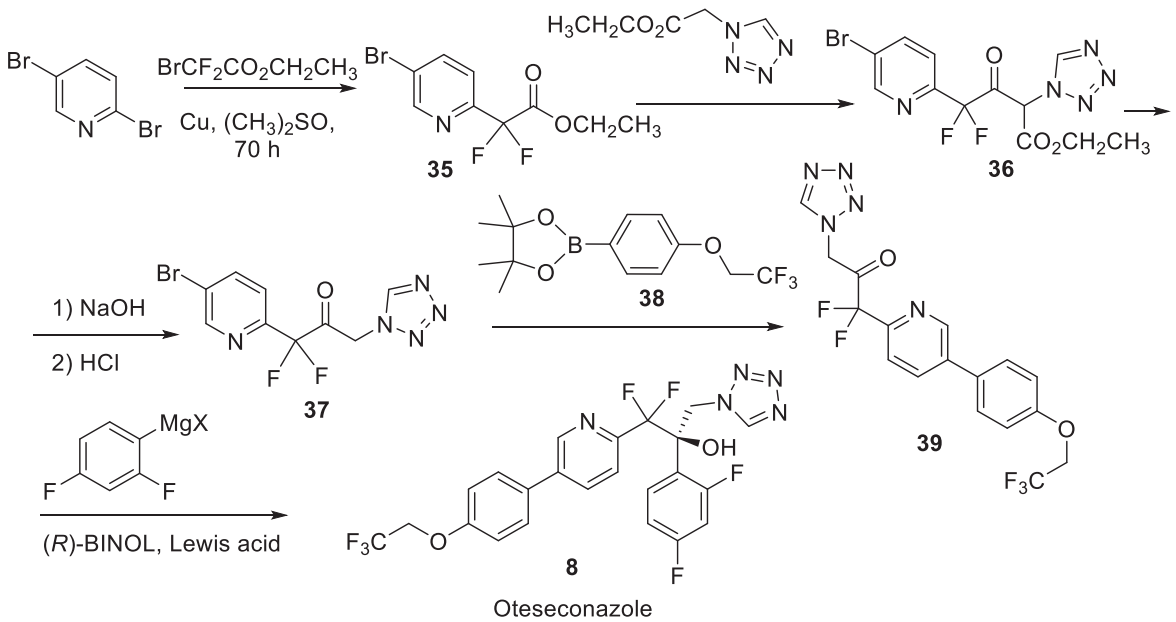

Scheme 5. The synthesis of Oteseconazole **8** starting from 2,5-dibromopyridine.

Compound **39** can also be prepared starting from 5-bromo-2-pyridinecaldehyde (Scheme 6). Suzuki coupling reaction of 5-bromo-2-pyridinecaldehyde with dioxaborolane **38** yields trifluoroethoxy aldehyde **40**. Subsequently, intermediate **40** is converted to difluoromethyl derivative **41** by reaction with (diethylamino)sulfur trifluoride. Finally, **41**, in the presence of strong base, is reacted with reagent **42** to yield **39** [147].

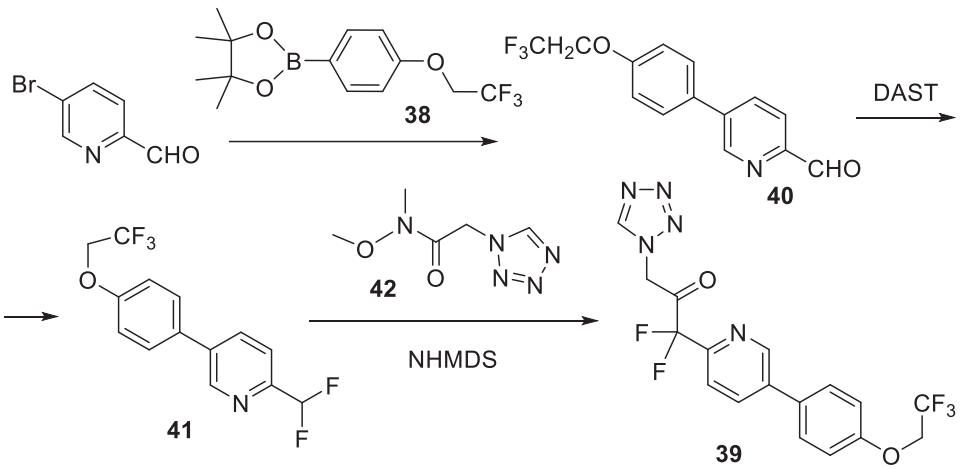

Scheme 6. The synthesis of the key difluoro ketone **39**. Legend: DAST, (diethylamino)sulfur trifluoride; NHMDS, sodium bis(trimethylsilyl)amide.

Oteseconazole **8** can be obtained enantiomerically pure by chiral HPLC [148]. In this regard, it is interesting to note a very recent breakthrough development in chiral purifications, *viz.* achiral simulated moving bed chromatography [149] leveraging the SDE phenomenon [150–152].

Sunlenca™ (Lenacapavir) ***9****.*

HIV/AIDS continues to be a major concern due to the rise of multidrug resistance and the challenges patients face in sticking to their treatment regimens [153]. There is currently no cure for HIV or AIDS. The HIV-1 capsid protein plays a crucial role in the viral replication cycle by protecting the virus's genetic material and other enzymes [154, 155]. Unlike earlier antiretroviral drugs that target protease, reverse transcriptase, and integrase, the capsid protein functions through protein–protein interactions making it a key target for novel drug design [156]. The capsid protein, along with Gag and Gag-Pol polyproteins, facilitates crucial interactions required for virion assembly [157]. The self-assembly of the capsid protein in the virion, which is responsible for the virus's infectivity, is initiated by cleavage mediated by HIV-1 protease [157, 158]. Additionally, the infection of a new cell is regulated by interactions with various host factors that support reverse transcription and proviral DNA integration [159–161]. Lenacapavir **9** is a groundbreaking HIV medication known as a capsid inhibitor. Developed by Gilead Sciences, Lenacapavir **9** can be used in conjunction with other antiretroviral drugs as a biannual treatment regimen. In December 2022, the FDA approved Lenacapavir **9** for HIV-1

treatment in adults with multidrug-resistant HIV infection. It works by preventing the virus from replicating and consequently reducing the levels of viral particles in the body [162]. This compound features a difluorobenzyl ring that fits into the same phenylalanine–glycine binding pocket as polyadenylation specificity factor subunit 6 (CPSF6) and nucleoporin 153 (Nup153). This binding establishes strong hydrophobic and hydrogen bonding interactions, thereby disrupting the interactions of capsid protein with Nup153 and CPSF6 [163–167]. By any measure, Lenacapavir **9** is a structurally unique pharmaceutical as it contains 10 fluorine atoms, representing four types of fluorination, and features three stereogenic centers.

The synthesis of the key intermediate **47** for the preparation of Lenacapavir **9** is presented in Scheme 7 [168]. The bicyclic ketone **43** is treated with lithium bis(trimethylsilyl)amide and ethyl trifluoroacetate to generate enolate **44**. The reaction of **44** with *N*-aminoglycine under Knorr pyrazole synthesis conditions affords **45**. The heterocyclic compound **45** is oxidized with *N*-hydroxyphthalimide and $NaClO_2$ to yield ketone **46**. Compound **46** is subjected to deoxyfluorination to afford the target **47**. Enantiomerically pure **47** is then obtained by chiral supercritical fluid chromatography.

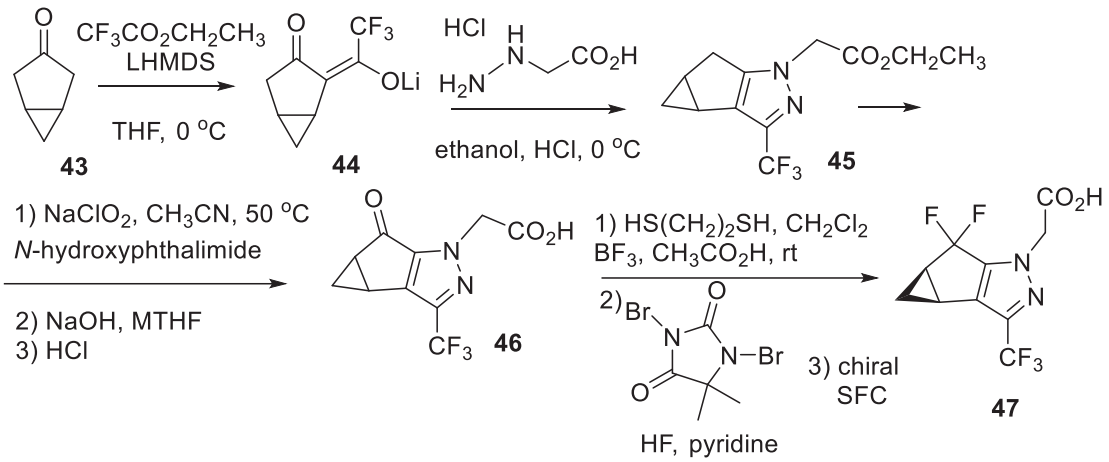

Scheme 7. The synthesis of key compound **47**. Legend: LHMDS, lithium bis(trimethylsilyl)amide; MTHF, 2-methyl tetrahydrofuran; SFC, supercritical fluid chromatography .

The synthesis of Lenacapavir **9** is illustrated in Scheme 8. Enantiomerically pure imine **48**, bearing an Ellman chiral auxiliary [169–172], undergoes reaction with the corresponding difluorobenzyl zinc reagent to provide amine **49**. Compound **49** is then subjected to Sonogashira coupling to afford product **50**. Next, Suzuki coupling is used to transform **50** to **52** using reagent **51**. The key intermediate, compound **47**, bearing a free carboxylic group, and amino compound **52** are reacted under peptide bond forming conditions to produce Lenacapavir **9**.

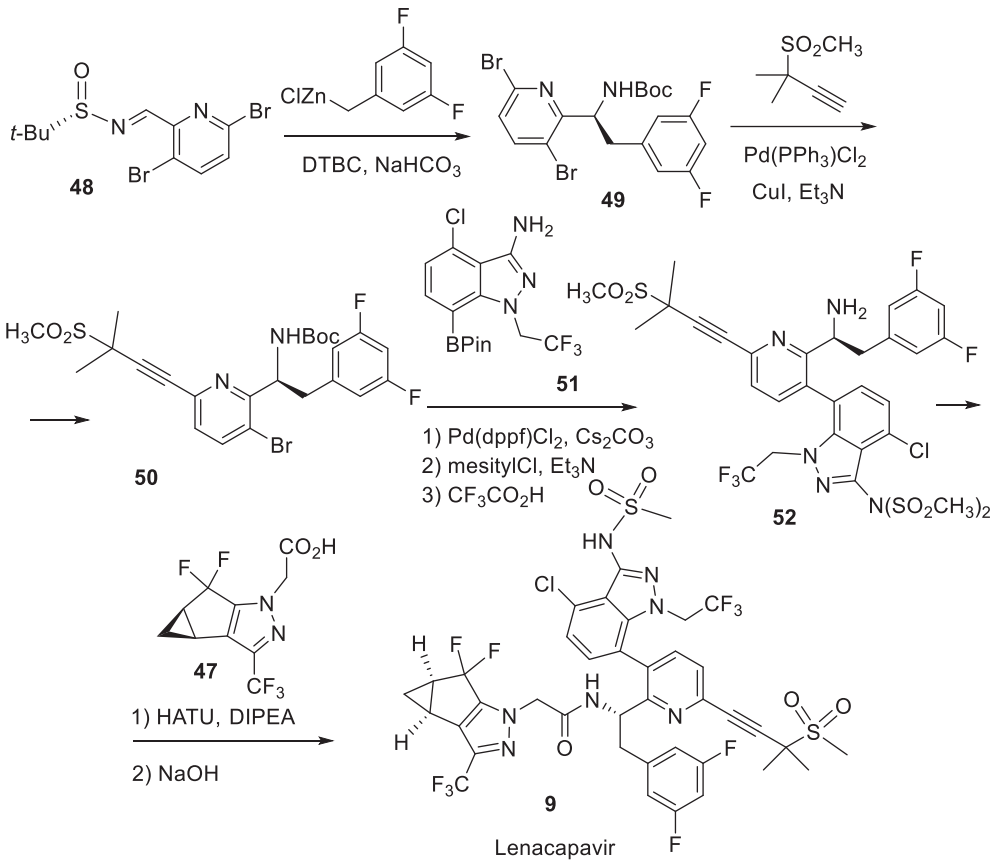

Scheme 8. The synthesis of Lenacapavir **9**. Legend: DIPEA, diisopropylethylamine; DTBC, di-*tert*-butyl decarbonate; HATU, hexafluorophosphate azabenzotriazole tetramethyl uranium.

*Voydeya® (Danicopan) **10**.*

Voydeya® **10**, marketed under the name Danicopan, is structurally derived from γ-fluorine-substituted proline with the fluorine atom directly bonded to the stereogenic carbon. Approved by the FDA on March 29th, 2024 it was developed by Alexion Pharmaceuticals, a subsidiary of AstraZeneca. Voydeya® **10** is specifically designed to address rare diseases, aligning with Alexion's specialization in orphan drug development [173]. Cyclic amino acids, such as proline and its derivatives used in the design of Voydeya® **10**, play a crucial role in drug development due to their increased steric constraints compared to linear analogs [174, 175]. Incorporating a fluorine atom or $-CF_3$ groups into five-membered rings [176–178] further limits conformational flexibility, allowing precise modulation of biological properties. Specifically, introducing a fluorine atom into the pyrrolidine-2-carboxamide framework, in contrast to non-fluorinated analogs like compounds **53** and **54** (Fig. 7), significantly enhances activity, *e.g.* achieving an impressive IC_{50} of 0.027 μM. This modification highlights exceptional potency and positions the compound as a leading candidate within its class [179, 180].

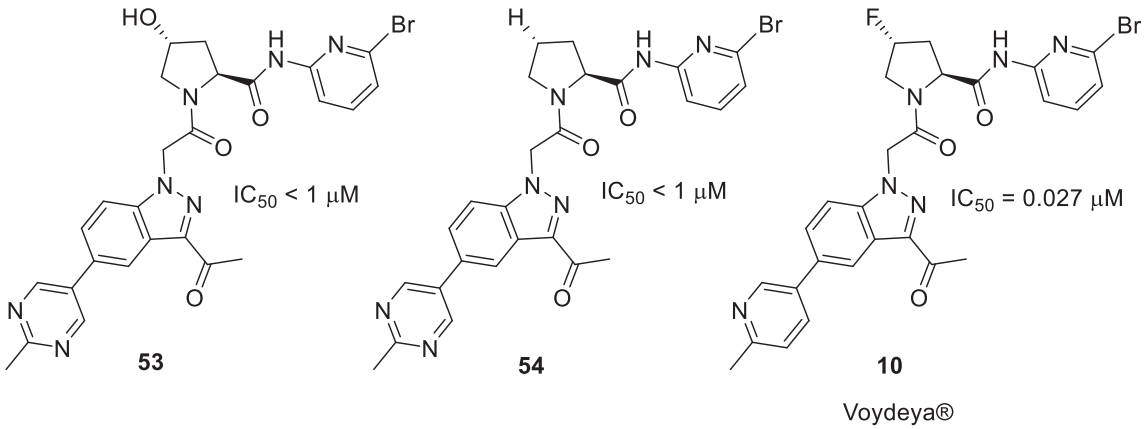

Figure 7. The structures of Voydeya® **10** and its fluorine-free analogs.

Voydeya® **10**, an oral complement Factor D inhibitor, is used as an add-on therapy to the complementary C5 inhibitors Ravulizumab and Eculizumab for treating extravascular hemolysis in adults with paroxysmal nocturnal hemoglobinuria (PNH) [181, 182]. PNH is a rare disorder in which the immune system's complement pathway attacks red and white blood cells as well as platelets, causing intravascular hemolysis and increasing the risk of thrombosis and organ damage. While C5 inhibitors are the standard treatment, some patients continue to experience residual extravascular hemolysis and anemia [183]. Voydeya® **10** was first approved in Japan on January 18th, 2024 for use in combination with C5 inhibitors to treat adults with PNH [184]. On February 23rd, 2024 the European Medicines Agency also recommended its use for patients with residual hemolytic anemia despite undergoing C5 inhibition therapy [185].

The synthesis of Voydeya® **10** [186–188] begins with the formation of several key intermediates. As depicted in Scheme 9, 5-bromo-1*H*-indazole-3-carbonitrile **53** undergoes reaction with methylmagnesium bromide generating an imine magnesium salt intermediate. Subsequent acid treatment at pH 5 hydrolyzes this intermediate yielding ketone **54**. The process continues with a Michael addition, resulting in ester **55** in 81% yield.

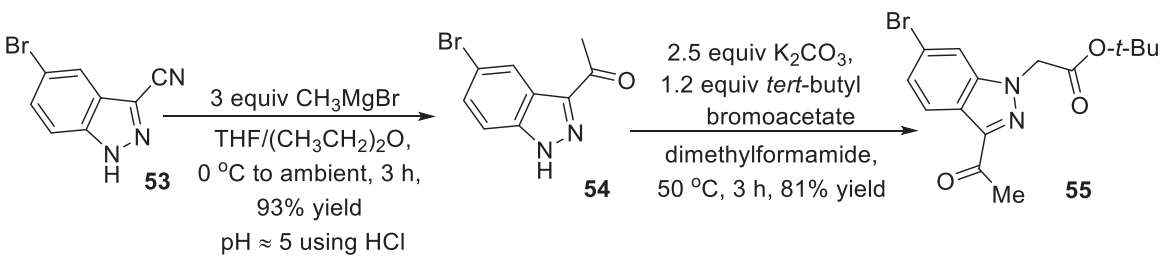

Scheme 9. The synthesis of intermediate **55**. Legend: THF, tetrahydrofuran.

The synthesis of another key intermediate, compound **58**, is depicted in Scheme 10. Boc-protected fluoropyrrolidine **56** undergoes amide alkylation using the Ghosez reagent and diisopropylethylamine [134] followed by deprotection of the amino group in **57** to afford precursor **58**.

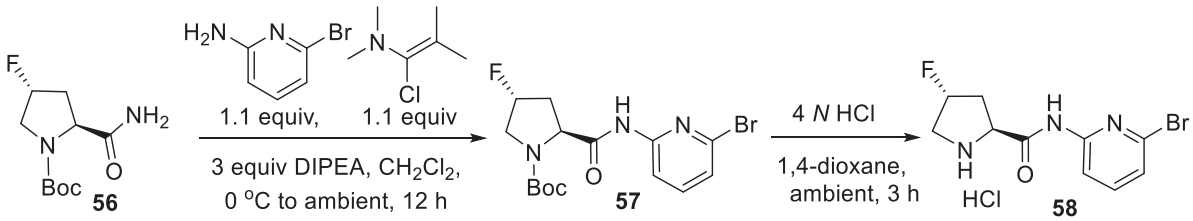

Scheme 10. The synthesis of intermediate **58**. Legend: Boc, *tert*-butyloxycarbonyl; DIPEA, diisopropylethylamine.

The final assembly of Voydeya® using the key intermediates **55** and **58** is illustrated in Scheme 11. Bromide **55** is reacted with boronate **59** to yield diester **60**. The second step involves palladium-catalyzed Suzuki–Miyaura coupling resulting in bis-aryl derivative **62**. Hydrolysis of the ester function using trifluoroacetic acid yields the free carboxylic acid **63**. The closing peptide coupling reaction using previously prepared fluoro proline derivative **58** affords Voydeya® **10**.

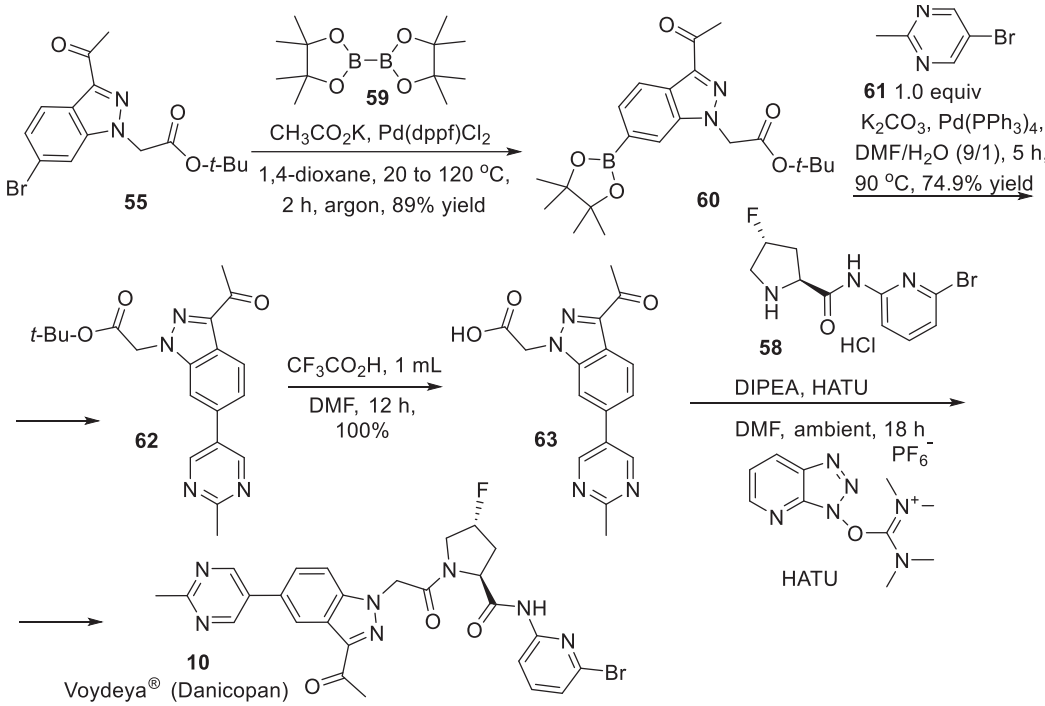

Scheme 11. The synthesis of Voydeya® **10**. Legend: DIPEA, diisopropylethylamine; DMF, dimethylformamide; HATU, hexafluorophosphate azabenzotriazole tetramethyl uranium.

Jaypirca® (Pirtobrutinib) ***11***.

Eli Lilly's Pirtobrutinib **11** is a highly selective and reversible Bruton's tyrosine kinase (BTK) inhibitor that can be administered orally [189]. BTK is crucial for the growth, activation, and survival of B cells, a type of white blood cell responsible for antibody production. However, uncontrolled B cell growth can lead to cancer [189]. Unlike the previously approved BTK inhibitor Ibrutinib **64** (Fig. 8), which binds irreversibly to the C481 residue in the kinase domain of BTK, Pirtobrutinib **11** offers a non-covalent, reversible inhibition method [190]. This unique mechanism makes Pirtobrutinib **11** effective in treating ibrutinib-resistant chronic lymphocytic leukemia that arises due to mutations in the C481 kinase domain [191].

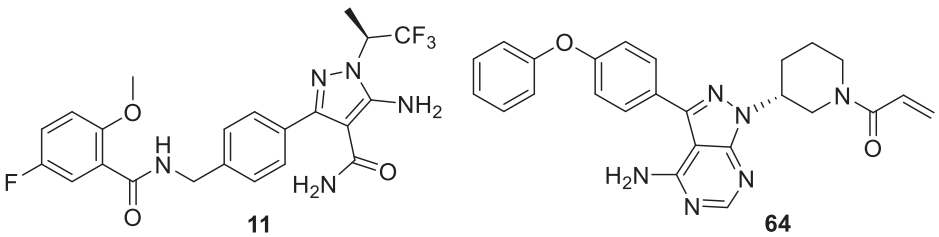

Figure 8. The structures of the clinically approved BTK inhibitors Pirtobrutinib **11** and Ibrutinib **64**.

Pirtobrutinib **11** features an aminopyrazole carboxamide ring, replacing the 4-aminopyrazolopyrimidine core of Ibrutinib **64**. The pyrazole ring acts as an ATP analog, binding competitively to the ATP binding site of BTK and ensuring the proper conformation for effective inhibition. Additionally, the covalent binding region of Ibrutinib **64** has been modified to a non-covalently bonded CF_3-substituted ethyl group.

In January 2023, the FDA approved Pirtobrutinib **11** for treating adult patients with relapsed or refractory mantle cell lymphoma following at least two lines of systemic therapy, including a BTK inhibitor [192, 193].

Eli Lilly's approach to synthesize Pirtobrutinib **11**, guided by Loxo Oncology, involves the preparation of two key intermediates: aminopyrazole derivative **65** (Scheme 12) and potassium trifluoroborate salt **66** (Scheme 13) [194, 195]. The meticulous process requires the synthesis of aminopyrazole derivative **65** and begins with the reaction between acid chloride **67** and malononitrile catalyzed by diisopropylethylamine. This is followed by O-methylation of the resulting 2-(hydroxymethylene)malononitrile derivative **68** using dimethyl sulfate, forming the 2-(methoxymethylene)malononitrile derivative **69**. Subsequent cyclization with (*S*)-(2,2,2-trifluoro-1-methyl)ethylhydrazine hydrochloride in the presence of triethylamine in ethanol at 80 °C yields aminopyrazole derivative **65** in an impressive 91% yield.

The synthesis of potassium trifluoroborate salt **66** (Scheme 13) starts with the reaction of pinacol bromomethyl boronic ester **70** with the sterically hindered potassium bis(trimethylsilyl)amide, resulting in silylated amino boronic ester **71**. This compound is then desilylated under mild conditions using methanol,

followed by acylation with acid chloride **72** to yield the amido boronic ester **73**. The cleavage of this pinacol boronic ester **73** using potassium bifluoride in a methanol/H_2O mixture at room temperature yields the desired potassium trifluoroborate salt **66**.

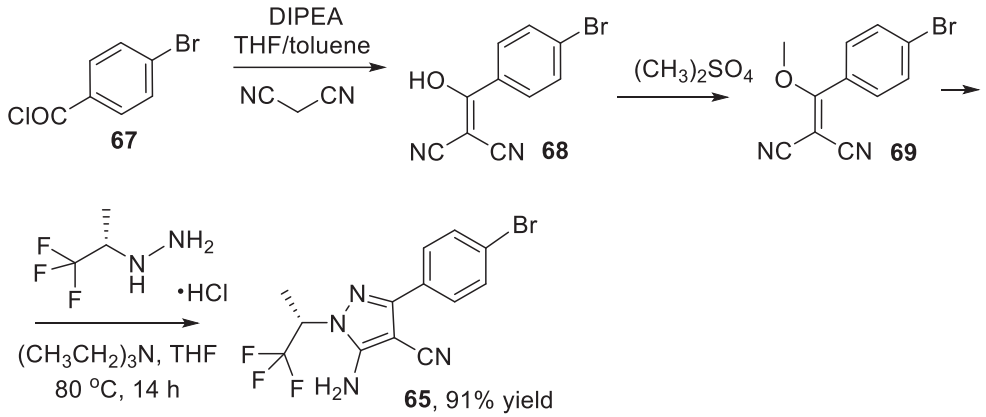

Scheme 12. The synthesis of compound **65**. Legend: DIPEA, diisopropylethylamine; THF, tetrahydrofuran.

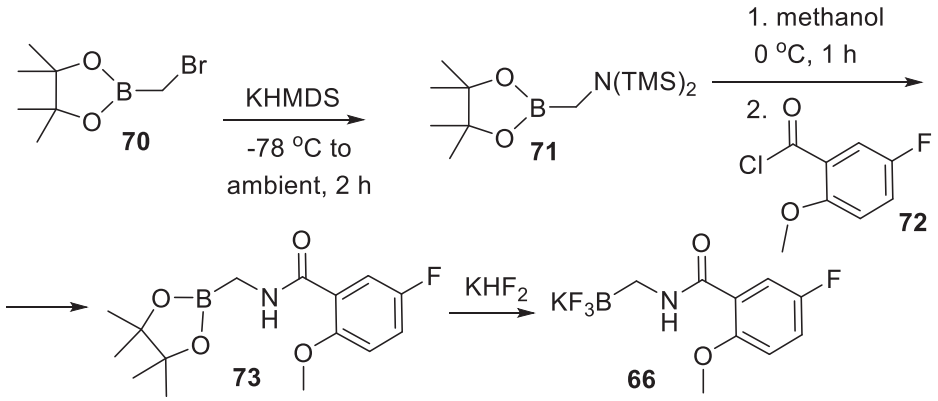

Scheme 13. The synthesis of compound **66**. Legend: KHMDS, potassium bis(trimethylsilyl)amide; TMS, trimethylsilyl.

The culmination of these efforts is the palladium-catalyzed cross-coupling reaction of aryl bromide **65** with potassium trifluoroborate salt **66** (Scheme 14). This reaction, facilitated by $Pd(OAc)_2$ as the precatalyst, Xphos as the ligand, and Cs_2CO_3 as the base in a tetrahydrofuran/H_2O mixture at 85 °C, yields the target 5-aminopyrazole-4-carbonitrile **74** in 87% yield after flash column chromatography over silica gel. The final step involves the hydrolysis of **74** using a solution of sulfuric acid and trifluoroacetic acid at 55 °C followed by flash column chromatography over silica gel, yielding Pirtobrutinib **11** as a white solid in 51% yield.

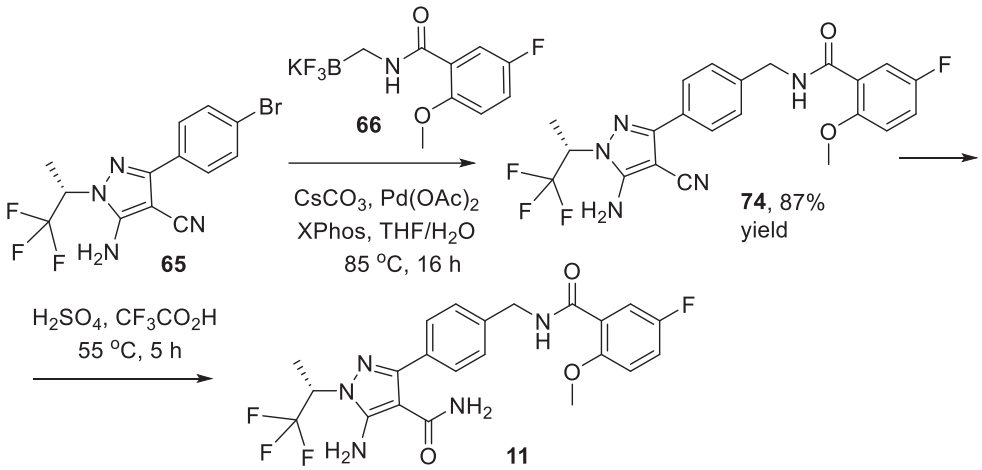

Scheme 14. The synthesis of Pirtobrutinib **11** by combining intermediates **65** and **66**. Legend: DIPEA, diisopropylethylamine; THF, tetrahydrofuran.

*Itovebi® (Inavolisib) **12**.*

Inavolisib **12**, known commercially as Itovebi®, has received FDA approval for the treatment of locally advanced or metastatic breast cancer [196]. This innovative drug acts as an inhibitor of the phosphatidylinositol-4,5-bisphosphate 3-kinase (PI3K) pathway, marking a new era of cancer therapeutics. It boasts an enhanced toxicity profile, surpassing that of its predecessor, alpelisib [197, 198].

PI3K enzymes are vital players in the orchestration of cell growth and differentiation, comprising both regulatory and catalytic subunits [199]. These enzymes come in four distinct isoforms: PI3Kα, PI3Kβ, PI3Kγ, and PI3Kδ. Of these, PI3Kα stands out as the most closely tied to cancer development thanks to mutations in the PIK3CA gene that encodes the p110α unit [200, 201]. Remarkably, nearly one third of breast cancer cases display such pathway anomalies [202], often marking a bleak prognosis [203].

The pursuit of selective PI3Kα inhibitors which circumvent the side effects associated with blocking other PI3K isoforms is a top priority [201–203]. Inavolisib **12** is a true virtuoso in this regard with an IC_{50} of only 0.034 nM for PI3Kα in comparison to 100 nM for PI3Kβ, 18 nM for PI3Kγ, and 12 nM for PI3Kδ. Inavolisib **12** thus exhibits an impressive 350-fold selectivity for PI3Kα [204]. Moreover, Inavolisib **12** also promotes the degradation of the mutated p110α subunit [205]. **12**'s precise targeting and high selectivity underscore a significant leap forward in the fight against breast cancer, offering hope and potential for more effective treatments.

It is intriguing to note that introducing a trifluoromethyl group in compound **75** (Fig. 9) leads to a PI3Kα IC_{50} of 0.095 nM and a PI3Kδ/PI3Kα ratio of 171, showing reduced selectivity for the α isoform. By contrast, with a difluoromethyl group, Inavolisib **12** exhibits a PI3Kα IC_{50} of 0.034 nM and a PI3Kδ/PI3Kα ratio of 361, highlighting a much higher selectivity for PI3Kα [206].

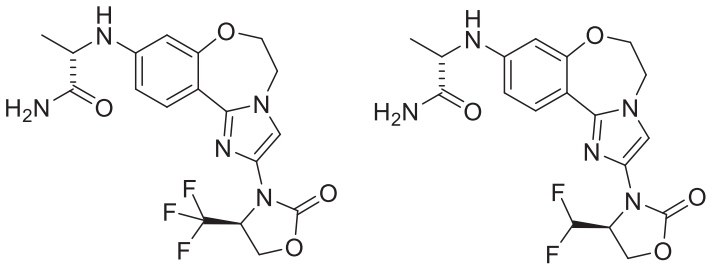

75

PI3Kα = 0.095 nM;
PI3Kδ/PI3Kα ratio = 171

12
Inavolisib

PI3Kα = 0.034 nM;
PI3Kδ/PI3Kα ratio = 361

Figure 9. The structures of Inavolisib **12** and its CF_3-containing analog **75**.

From a chemical perspective, Inavolisib **12** is comprised of a benzoxazepine oxazolidinone core adorned with an alanine amide moiety and an amino alcohol derived from difluoroalanine. This particular difluoroalanine derivative is highly attractive to PI3Kα, significantly boosting the drug's selectivity for this isoform. The efficacy of **12**'s interactions with its target is enhanced by hydrogen bonds formed between the amide and amino groups of the alanine fragment. Furthermore, the difluoromethyl group of Inavolisib **12** engages with the hydroxyl group of Ser774 within the p110α pocket [204]. Hence, strategic fluorination is the key to the high potency of this PI3Kα inhibitor.

The synthesis of Inavolisib **12** (Scheme 15) begins with 1,2:5,6-*bis*-*O*-(1-methylethylidene)-D-mannitol (**76**) to provide the desired stereochemical configuration [206]. The process begins with sodium periodate in hot water which is added to silica to form a powder that is combined with compound **30** dissolved in dichloromethane. After stirring at room temperature for an hour, carbaldehyde **77** is produced. As the reaction cools, diethylaminosulfur trifluoride is gradually added to the carbaldehyde **77** solution in dichloromethane, which is then stirred at room temperature for three hours to produce (*R*)-4-difluoromethyl-2,2-dimethyl[1,3]dioxolane (**78**). Intermediate **78** is dissolved in methanol and hydrochloric acid in dioxane is added followed by stirring at room temperature for 30 minutes. The acetal is cleaved to form the respective diol. Following work up, the residue is dissolved in dichloromethane followed by the addition of *tert*-butyldimethylsilyl chloride, triethylamine, and a catalytic amount of 4-dimethylaminopyridine. After stirring for an hour at room temperature, compound **79** is obtained. The next step involves adding trifluoromethanesulfonic anhydride dropwise to a solution of **79** and pyridine in dichloromethane. The temperature is maintained at −20 °C for 20 minutes then brought to 0 °C for an hour while stirring. After extraction and work up, the residue is dissolved in dimethyl formamide and sodium azide is added followed by stirring for two hours at room temperature to produce intermediate **80**. Azide **80** is then reduced using

palladium hydroxide on carbon under hydrogen by stirring for 16 hours in ethyl acetate and methanol, yielding primary amine **81**. This product is dissolved in methanol and stirred in a solution of HCl in dioxane for two hours at room temperature to remove the protecting group. After work up, the crude product is dissolved in toluene and aqueous potassium hydroxide at 0 °C. Phosgene is added gradually, followed by stirring for an hour to obtain (*S*)-4-difluoromethyloxazolidin-2-one (**82**). This is then combined with 9-bromo-2-iodo-5,6-dihydrobenzo[*f*]imidazo[1,2-*d*][1,4]-oxazepane (**83**), copper acetate monohydrate, 3,4,7,8-tetramethyl-1,10-phenanthroline, and cesium carbonate in dioxane. The mixture is heated to 100 °C for 18 hours under an argon atmosphere resulting in compound **84** [206].

Compound **84** is then suspended in dimethyl sulfoxide with L-alanine, cuprous iodide, and potassium phosphate tribasic with heating at 100 °C for two hours. Once cooled to ambient temperature, dimethyl sulfoxide, ammonium chloride, and triethylamine are added. To this suspension, hexafluorophosphate azabenzotriazole tetramethyl uranium is added dropwise and stirred at room temperature for an hour to finally obtain Inavolisib **12** [206].

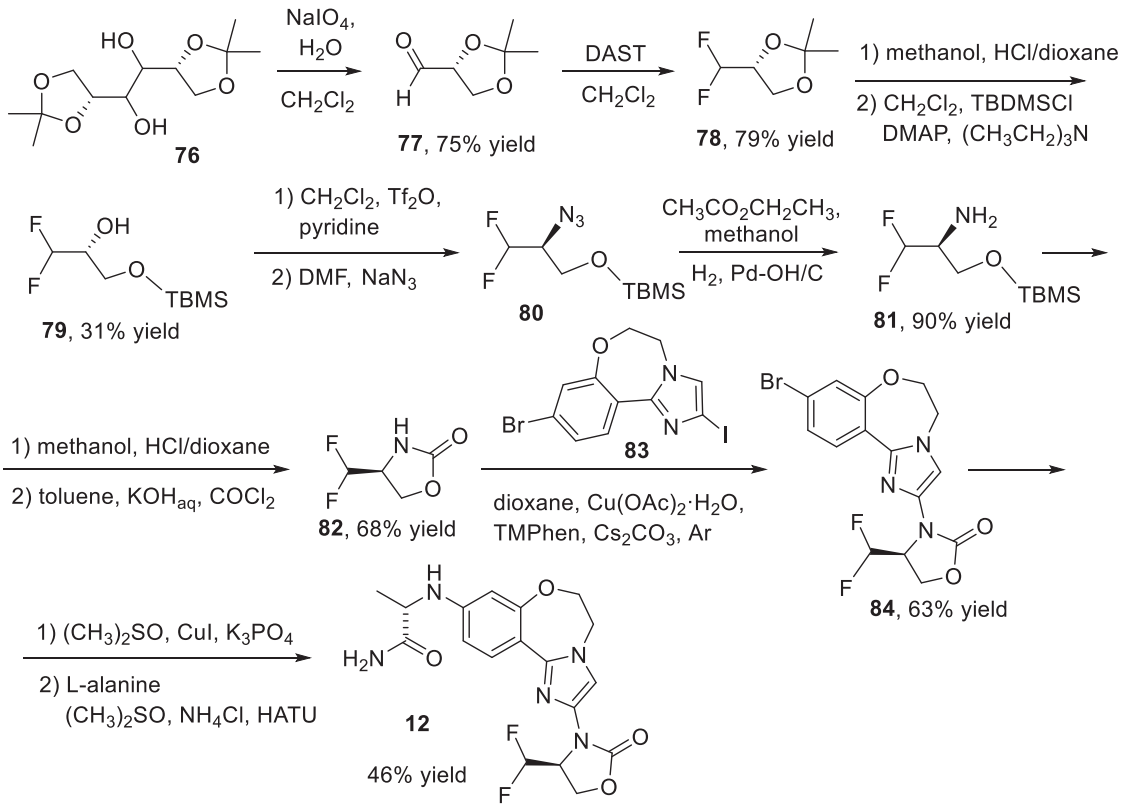

Scheme 15. The synthesis of Inavolisib **12**. Legend: DAST, (diethylamino)sulfur trifluoride; DMAP, 4-(dimethylamino)pyridine; DMF, dimethylformamide; HATU, hexafluorophosphate azabenzotriazole tetramethyl uranium; TBDMSCl, *tert*-butyl dimethyl silyl chloride; Tf_2O, trifluoromethanesulfonic anhydride; THF, tetrahydrofuran; TMPhen, 3,4,7,8-tetramethyl-1,10-phenanthroline.

Conclusions. Each of the nine compounds profiled in this review features a unique structural arrangement of fluorine with respect to the chirality of the molecule. Fluoroestradiol F-18 (Cerianna™) **4** has a single fluorine atom on the stereogenic carbon β to a hydroxy group. This unit is part of a five-membered ring, which is itself part of a polycyclic system possessing five consecutive stereogenic centers. Cedazuridine **17** features a difluoromethylene group as part of a tetrahydrofuran heterocyclic moiety bearing three additional amino, hydroxy, and hydroxymethyl substitutions on three stereogenic carbons. The molecule contains four centers of chirality overall. Belzutifan (Welireg™) **6** possesses a 1,2-difluoroethylene group as part of a dihydroindene system with a hydroxy group and a stereogenic center vicinal to one of the fluorine atoms. Each fluorine atom is directly bonded to a stereogenic carbon thus there are three consecutive chiral centers within the five-membered ring. Voranigo® (Vorasidenib) **7** has two trifluoromethyl groups as fragments of chiral trifluoro-isopropylamine moieties, which sterically and electronically influence the properties of the amino groups. Vivjoa™ (Oteseconazole) **8** features an acyclic difluoromethylene group bonded directly to a quaternary stereogenic carbon. Additionally, the molecule includes two aromatic fluorine substitutions and a trifluoroethoxy group. In Sunlenca™ (Lenacapavir) **9**, the difluoromethylene group is bonded to a stereogenic center as part of a highly sterically constrained tricyclic system composed of one three-membered and two five-membered rings. The molecule possesses two aromatic fluorines, one aromatic trifluoromethyl, and one trifluoroethyl substitution and has three centers of chirality overall. Voydeya® (Danicopan) **10** features a monofluoroproline residue as a centerpiece of its structure and is the fluorinated analog of natural occurring hydroxyproline, a compound which is essential for collagen structure and function. The molecule has two stereogenic centers within the glycine-fluoroproline dipeptide unit. Jaypirca® (Pirtobrutinib) **11** includes a trifluoromethyl group bonded to the stereogenic center of a trifluoropropanylhydrazine structural fragment. Finally, Itovebi® (Inavolisib) **12** possesses a chiral oxazolidinone ring with a difluoromethyl group bonded to the stereogenic carbon. The second stereogenic center in the molecule is associated with an alanine residue.

This diverse array of chiral, fluorine substitutions shows that there is currently no established structurally favored pattern in the design of modern drugs. Consequently, there remains a need for the synthesis of a variety of chiral, fluorine molecules for data collection, analysis, and theoretical predictions. It is well established that incorporating elements of chirality, particularly a stereogenic center, in compounds under development enhances their success rate as they progress from discovery to marketing approval. For example, approximately 65% of approved drugs have at least one element of chirality, compared to about 50% of candidates in the discovery phase [207]. Therefore, it is anticipated that chiral, fluorine-containing compounds will continue to play an indispensable role in modern medicinal chemistry, becoming even more prominent in the drug candidates being designed, developed, and submitted for approval.

We gratefully acknowledge the financial support from the National Natural Science Foundation of China (No. 21761132021), the Qing-Lan Project of Jiangsu Province (for Han), and IKERBASQUE, Basque Foundation for Science (for Soloshonok).

ХІРАЛЬНІ ФАРМАЦЕВТИЧНІ ПРЕПАРАТИ, ЩО МІСТЯТЬ ФТОР

Ц. Хань,[1] А. Взорек,[2] Г. Дхаван,[3,4] В. Зханг,[5] О. Є. Сорочинський,[6] Д. Бекер,[7] Т. Оно,[8] К. Д. Клика,[9] В. А. Солошонок[10,11]*

[1]Спільний інноваційний центр Цзянсу з ефективного оброблення та використання лісових ресурсів, Коледж хімічної інженерії, Нанкінський лісотехнічний університет, Нанкін 210037, Китай;
[2]Інститут хімії, Університет імені Яна Кохановського в Кельцях, Кельці, Польща;
[3]Школа медичних наук, Університет підприємництва Делі, Нью-Делі-110077, Індія;
[4]Коледж Ачаріа Нарендра Дев, Університет Делі, Нью-Делі 110019, Індія;
[5]Департамент хімії, Массачусетський університет, Бостон, Массачусетс 02125, США;
[6]Інститут біоорганічної хімії та нафтохімії ім. В.П. Кухаря НАН України,
Київ, Україна;
Адреса!
[7]Департамент фармацевтичної та медичної хімії, Інститут фармації, Вільний університет Берліна, 14195 Берлін, Німеччина;
[8]Національний інститут передових промислових наук і технологій, 463–8560, Нагоя, Японія;
[9] Центр досліджень і розробок,
Archer Daniels Midland, 1001 N Brush College Rd., Декейтер, Іллінойс 62521, США;
[10]Хімічний факультет, Університет Країни Басків, 20018 Сан-Себастьян, Іспанія;
[11] ІКЕРБАСК, Баскський фонд науки, 48013 Більбао, Іспанія

**email: vadimsoloshonok@gmail.com*

Фтор, відомий своїми унікальними хімічними властивостями, став ключовим елементом у розробленні лікарських засобів завдяки його здатності підвищувати метаболічну стабільність, покращувати спорідненість зв'язування та збільшувати біодоступність. Ця стаття досліджує останні досягнення у сфері хіральних фармацевтичних препаратів, що містять фтор, які було введено на ринок за останні п'ять років, зосереджуючись на їхньому синтезі, терапевтичних перевагах, механізмах дії та впливу фтору на їхню ефективність та профіль безпеки. Через огляд хіральних препаратів, нещодавно схвалених FDA, ми прагнемо надати уявлення про розвиток хімії фтору у розробленні лікарських засобів та її значення для майбутніх терапевтичних інновацій. Наголошено на необхідності більшого дослідження явища самодиспропорціонування енантіомерів (SDE) у хіральних фторвмісних сполуках. Зазначено надмірний рівень фтору як у навколишньому середовищі, так і у життєдіяльності людей.

Ключові слова: фтор, хіральність, фармацевтичні препарати, розроблення лікарських засобів, синтез, SDE, біоактивність.

REFERENCES

[1] Malerba F., Orsenigo L. The evolution of the pharmaceutical industry. *Bus. Hist*. 2015. **57**(5): 664–687. doi.org/10.1080/00076791.2014.975119.
[2] Goodman J. *Pharmaceutical industry*. In *Medicine in the twentieth century*. Taylor & Francis. 2020. pp. 141–154. ISBN 9781003078456.
[3] Horrobin D. F. Innovation in the pharmaceutical industry. *J. Roy. Soc. Med*. 2000. **93**(7): 341–345.

doi.org/10.1177/014107680009300.
[4] Cockburn I. M. The changing structure of the pharmaceutical industry. *Health Affair*. 2004. **23**(1): 10–22. doi.org/10.1377/hlthaff.23.1.10.
[5] Comanor W. S. The political economy of the pharmaceutical industry. *J. Econ Lit*. 1986. **24**(3): 1178–217. https://www.jstor.org/stable/2725866.
[6] Hutt A. J., Tan S. C. Drug Chirality and its Clinical Significance. *Drugs*. 1996. **52** (Suppl 5): 1–12. doi.org/10.2165/00003495-199600525-00003.
[7] Lin G. Q., You Q. D., Cheng J. F. *Chiral drugs*. In *Chemistry and Biological Action*. Wiley, 2011. doi:10.1002/9781118075647.
[8] Brooks W. H., Guida W. C., Daniel K. G. The significance of chirality in drug design and development. *Curr. Top. Med. Chem*. 2011. **11**(7): 760–770. doi: 10.2174/156802611795165098.
[9] Ceramella J., Iacopetta D., Franchini A. *et al*. A look at the importance of chirality in drug activity: Some significative examples. *Appl. Sci*. 2022. **12**(21): 10909. doi.org/10.3390/app122110909.
[10] Crossley R. J. *Chirality and biological activity of drugs*. CRC Press, 1995.
[11] Calcaterra A., D'Acquarica I. The market of chiral drugs: Chiral switches versus de novo enantiomerically pure compounds. *J. Pharmaceut. Biomed. Anal*. 2018. **147**: 323–340. doi.org/10.1016/j.jpba.2017.07.008.
[12] Wang J., Sánchez-Roselló M., Aceña J. L. *et al*. Fluorine in pharmaceutical industry: Fluorine-containing drugs introduced to the market in the last decade (2001–2011). *Chem. Rev*. 2014. **114**(4): 2432–2506. doi: 10.1021/cr4002879.
[13] Zhou Y., Wang J., Gu Z. *et al*. Next Generation of Fluorine-Containing Pharmaceuticals, Compounds Currently in Phase II–III Clinical Trials of Major Pharmaceutical Companies: New Structural Trends and Therapeutic Areas. *Chem. Rev*. 2016. **116**(2): 422–518. doi: 10.1021/acs.chemrev.5b00392.
[14] Han J., Remete A. M., Dobson L. S. *et al*. Next generation organofluorine containing blockbuster drugs. *J. Fluor. Chem*. 2020. **239**: 109639. doi: 10.1016/j.jfluchem.2020.109639.
[15] O'Hagan D. Fluorine in health care: Organofluorine containing blockbuster drugs. *J. Fluor. Chem*. 2010. **131**(11): 1071–1081. doi.org/10.1016/j.jfluchem.2010.03.003.
[16] Strunecká A., Patočka J., Connett P. Fluorine in medicine. *J Appl Biomed*. 2004. **2**: 141–150. ISSN 1214 0287.
[17] Soloshonok V. A., Kirilenko A. G., Kukhar V. P., Resnati G. Transamination of fluorinated β-keto carboxylic esters. A biomimetic approach to β-polyfluoroalkyl-β-amino acids. *TetrahedronLett*. 1993. **34**(22): 3621–3624. doi: 10.1016/S0040-4039(00)73652-5.
[18] Hagmann W. K. The many roles for fluorine in medicinal chemistry. *J. Med. Chem*. 2008. **51**(15): 4359–4369. doi.org/10.1021/jm800219f.
[19] Gupta S. P. Roles of fluorine in drug design and drug action. *Lett. Drug Des. Discov*. 2019. **16**(10): 1089–1109. doi: 10.2174/1570180816666190130154726.
[20] Ye Z., Zhao G. Asymmetric Synthesis of Fluorine-containing Compounds Using Organocatalysts. *Chimia*. 2011. **65**: 902. doi: 10.2533/chimia.2011.902.
[21] Cahard D., Bizet V. The influence of fluorine in asymmetric catalysis. *Chem. Soc. Rev*. 2014. **43**(1):135–147.
[22] Bizet V., Cahard D. Fluorine as a control element in asymmetric synthesis. *Chimia*. 2014. **68**: 378. doi: 10.2533/chimia.2014.378.
[23] Yamada T., Okada T., Sakaguchi K. *et al*.Efficient asymmetric synthesis of novel 4-substituted and configurationally stable analogues of thalidomide. *Org. Lett*. 2006. **8**(24): 5625–5628. doi: 10.1021/ol0623668.

[24] Shibata N., Nishimine T., Shibata N. *et al*. Organic base-catalyzed stereodivergent synthesis of (*R*)- and (*S*)-3-amino-4,4,4-trifluorobutanoic acids. *Chem*. *Commun*. 2012. **48**(34): 4124–4126.
doi: 10.1039/C2CC30627A.

[25] Soloshonok V. A., Hayashi T. Gold(I)-catalyzed asymmetric aldol reaction of fluorinated benzaldehydes with α-isocyanoacetamide. *Tetrahedron*: *Asymmetry.* 1994. **5**(6): 1091–1094.
doi: 10.1016/0957-4166(94)80059-6.

[26] Ma J. A., Cahard D. Asymmetric fluorination, trifluoromethylation, and perfluoroalkylation reactions. *Chem. Rev*. 2004. **104**(12): 6119–6146.
doi: 10.1021/cr030143e.

[27] Soloshonok V. A., Kirilenko A. G., Fokina N. A. *et al*. Biocatalytic resolution of β-fluoroalkyl-β-amino acids. *Tetrahedron: Asymmetry.* 1994. **5**(6): 1119–1126.
doi: 10.1016/0957-4166(94)80063-4.

[28] Turcheniuk K. V., Poliashko K. O., Kukhar V. P. *et al*. Efficient asymmetric synthesis of trifluoromethylated β-aminophosphonates and their incorporation into dipeptides. *Chem*. *Commun*. 2012. **48**(94): 11519–11521.
doi: 10.1039/C2CC36702E.

[29] Welch J. T., Araki K., Kawecki R., Wichtowski J. A. Stereocontrol by the carbon-fluorine bond and its application to asymmetric synthesis of 3-fluoro. beta.-lactams. *J. Org. Chem*. 1993. **58**(9): 2454–2462.
doi.org/10.1021/jo00061a019.

[30] Zhu Y., Han J. L., Wang J.*et al*.Modern Approaches for Asymmetric Construction of Carbon–Fluorine Quaternary Stereogenic Centers: Synthetic Challenges and Pharmaceutical Needs. *Chem. Rev*. 2018. **118**(7): 3887–3964.
doi: 10.1021/acs.chemrev.7b00778.

[31] Bravo P., Capelli S., Meille S. V. *et al*. Synthesis of optically pure (*R*)- and (*S*)-α-trifluoromethyl-alanine. *Tetrahedron*: *Asymmetry*. 1994. **5**(10): 2009–2018.
doi: 10.1016/S0957-4166(00)86276-X.

[32] Sorochinsky A. E., Aceña J. L., Soloshonok V. A. Self-disproportionation of enantiomers of chiral, non-racemic fluoroorganic compounds: Role of fluorine as enabling element. *Synthesis*. 2013. **45**(2): 141–152.
doi: 10.1055/s-0032-1316812.

[33] Sorochinsky A. E., Katagiri T., Ono T. *et al*. Optical purifications via self-disproportionation of enantiomers by achiral chromatography; Case study of a series of α-CF_3-containing secondary alcohols. *Chirality*. 2013. **25**(6): 365–368.
doi: 10.1002/chir.22180.

[34] Soloshonok V. A., Berbasov D. O. Self-Disproportionation of Enantiomers on Achiral Phase Chromatography. One More Example of Fluorine's Magic Powers. *Chim. Oggi/ Chem. Today*. 2006. **24**: 44–47.

[35] Nakamura T., Tateishi K., Tsukagoshi S. *et al.* Self-disproportionation of enantiomers of non-racemic chiral amine derivatives through achiral chromatography. *Tetrahedron*. 2012. **68**(21): 4013–4017.
doi:10.1016/j.tet.2012.03.054.

[36] Yasumoto M., Ueki H., Ono T. *et al*. Self-disproportionation of enantiomers of isopropyl 3,3,3-(trifluoro)lactate via sublimation:Sublimation rates vs. enantiomeric composition. *J. Fluor. Chem*. 2010. **131**(4): 535–539.
doi.org/10.1016/j.jfluchem.2009.11.026.

[37] Suzuki Y., Han J., Kitagawa O. *et al*. A comprehensive examination of the self-disproportionation of enantiomers (SDE) of chiral amides *via* achiral, laboratory-routine, gravity-driven column chromatography. *RSC Adv*. 2015. **5**(4): 2988–2993.
doi: 10.1039/C4RA13928C.

[38] Soloshonok V. A., Wzorek A., Klika K. D. A question of policy: should tests for the self-disproportionation of enantiomers (SDE) be mandatory for reports involving scalemates? *Tetrahedron: Asymmetry*. 2017. **28**(10): 1430–1434.
doi: 10.1016/j.tetasy.2017.08.020.

[39] Han J., Kitagawa O., Wzorek A. *et al*. The self-disproportionation of enantiomers (SDE): a menace or an opportunity? *Chem. Sci*. 2018. **9**(7): 1718–1739. doi: 10.1039/C7SC05138G.

[40] Soloshonok V. A., Klika K. D. Terminology related to the phenomenon 'self-disproportionation of enantiomers' (SDE). *Helv. Chem. Acta*. 2014. **97**(11): 1583–1589. doi: 10.1002/hlca.201400122.

[41] Han J., Dembinski R., Soloshonok V. A., Klika K. D. A call for a change in policy regarding the necessity for SDE tests to validate the veracity of the outcome of enantioselective syntheses, the inherent chiral state of natural products, and other cases involving enantioenriched samples. *Molecules*. 2021. **26**(13): 3994. doi.org/10.3390/molecules26133994.

[42] Han J., Wzorek A., Klika K. D., Soloshonok V. A. Recommended tests for the self-disproportionation of enantiomers (SDE) to ensure accurate reporting of the stereochemical outcome of enantioselective reactions. *Molecules*. 2021. **26**(9): 2757. doi.org/10.3390/molecules26092757.

[43] Han J., Kiss L., Mei H. *et al*. Chemical aspects of human and environmental overload with fluorine. *Chem. Rev*. 2021. **121**(8): 4678–4742. doi: 10.1021/acs.chemrev.0c01263.

[44] Kabir H., Gupta A. K., Tripathy S. Fluoride and human health: Systematic appraisal of sources, exposures, metabolism, and toxicity. *Crit. Rev. Env. Sci. Tec*. 2020. **50**(11): 1116–1193. doi.org/10.1080/10643389.2019.1647028.

[45] Zuo H., Chen L., Kong M. *et al*. Toxic effects of fluoride on organisms. *Life Sci*. 2018. **198**: 18–24. doi.org/10.1016/j.lfs.2018.02.001.

[46] Ozsvath D. L. Fluoride and environmental health: a review. *Rev. Env. Sci. Bio*. 2009. **8**:59–79. doi: 10.1016/B978-0-444-53086-8.00012-6.

[47] Peckham S., Awofeso N. Water Fluoridation: A Critical Review of the Physiological Effects of Ingested Fluoride as a Public Health Intervention. *Sci. World J*. 2014. 293019. doi.org/10.1155/2014/293019.

[48] Smith G. E. Fluoride, the environment, and human health. *Perspect. Biol. Med*. 1986. **29**(4): 560–572. doi: 10.1353/pbm.1986.0028.

[49] Srivastava S., Flora S. J. Fluoride in Drinking Water and Skeletal Fluorosis: a Review of the Global Impact. *Curr. Env. Health Rep*. 2020. **7**(2):140–146. doi.org/10.1007/s40572-020-00270-9.

[50] Mei H., Han J., Fustero S.*et al*. Fluorine-Containing Drugs Approved by the FDA in 2018. *Chem.—Eur. J*. 2019. **25**(51): 11797–11819. doi: 10.1002/chem.201901840.

[51] Mei H., Remete A. M., Zou Y. *et al*. Fluorine-containing drugs approved by the FDA in 2019. *Chin. Chem. Lett*. 2020. **31**(9): 2401–2413. doi: 10.1016/j.cclet.2020.03.050.

[52] Wang Q., Bian Y., Dhawan, G. *et al*. FDA approved fluorine-containing drugs in 2023. *Chin. Chem. Lett*. 2024. **35**(11): 109780. doi: 10.1016/j.cclet.2024.109780.

[53] Han J., Wzorek A., Dhawan G. *et al*. New drugs on the pharmaceutical market containing fluorine and residues of tailor-made amino acids. Ukr. Chim. J. 2024. 90(9): 31–56.

[54] Yu Y., Liu A., Dhawan G. *et al*.Fluorine-containing pharmaceuticals approved by the FDA in 2020: Synthesis and biological activity. *Chin. Chem. Lett*. 2021. **32**(11): 3342–3354. doi: 10.1016/j.cclet.2021.05.042.

[55] He J., Li Z., Dhawan G. *et al*. Fluorine-containing drugs approved by the FDA in 2021. *Chin. Chem. Lett*. 2023. **34**(1): 107578. doi: 10.1016/j.cclet.2022.06.001.

[56] Wang Q., Han J., Sorochinsky A. *et al*. The Latest FDA-Approved Pharmaceuticals Containing Fragments of Tailor-Made Amino Acids and Fluorine. *Pharmaceuticals*. 2022. **15**(8): 999. doi.org/10.3390/ ph150809991847558.

[57] Schoepfer J., Jahnke, W., Berellini G. *et al*.,

Discovery of Asciminib (ABL001), an Allosteric Inhibitor of the Tyrosine Kinase Activity of BCR-ABL1. *J. Med. Chem*. 2018. **61**(18): 8120–8135.
doi.org/10.1021/acs.jmedchem.8b01040.

[58] Dhillon S., Melphalan flufenamide (Melflufen): first approval. *Drugs*. 2021. **81**(8): 963–969.
doi.org/10.6084/m9.figshare.14390954.

[59] Blair H. A. Sotorasib: first approval. *Drugs*. 2021. **81**(13): 1573–1579.
doi.org/10.6084/m9.figshare.15078999.

[60] Yin Z., Hu W., Zhang W. *et al*. Tailor-made amino acid-derived pharmaceuticals approved by the FDA in 2019. *Amino Acids*. 2020. **52**(9): 1227–1261.
doi: 10.1007/s00726-020-02887-4.

[61] Mei H., Han J., White S. *et al*. Tailor-made amino acids and fluorinated motifs as prominent traits in modern pharmaceuticals. *Chem.—Eur. J*. 2020. **26**(50): 11349–11390.
doi:10.1002/chem.202000617.

[62] Liu J., Han J., Izawa K. *et al*. Cyclic tailor-made amino acids in the design of modern pharmaceuticals. *Eur. J. Med. Chem*. 2020. **208**: 112736.
doi: 10.1016/j.ejmech.2020.112736.

[63] Han J., Konno H., Sato T., *et al*. Peptidomimetics and Peptide-Based Blockbuster Drugs. *Curr. Org. Chem*. 2021. **25**(14):1627–1658.
doi: 10.2174/1385272825666210610155047.

[64] Han J., Konno H., Sato T. *et al*.Tailor-made amino acids in the design of small-molecule blockbuster drugs. *Eur. J. Med. Chem*. 2021. **220**: 113448.
doi: 10.1016/j.ejmech.2021.113448.

[65] Liu A., Han J., Nakano A., *et al*. New pharmaceuticals approved by FDA in 2020: Small-molecule drugs derived from amino acids and related compounds. *Chirality*. 2022. **34**(1): 86–103.
doi: 10.1002/chir.23376.

[66] Wang N., Mei H., Dhawan G. *et al*. New Approved Drugs Appearing in the Pharmaceutical Market in 2022, Featuring Fragments of Tailor-Made Amino Acids and Fluorine. *Molecules*. 2023. **28**(9): 3651.
doi:10.3390/molecules28093651.

[67] Han J., Wzorek A., Dhawan G. *et al*.New drugs appearing on the market in 2023: molecules containing fluorine and fragments of tailor-made amino acids. *Ukr. Bioorg. Acta*. 2024. **19**(1): 3–20.
doi: 10.15407/bioorganica2024.01.003.

[68] Han J., Lyutenko N. V., Sorochinsky A. E., *et al*. Tailor-Made Amino Acids in Pharmaceutical Industry: Synthetic Approaches to Aza-Tryptophan Derivatives. *Chem.—Eur. J*. 2021. **27**(70): 17510–17528.
doi: 10.1002/chem.202102485.

[69] Park B. K., Kitteringham N. R., O'Neill P. M. Metabolism of fluorine-containing drugs. *Ann. Rev. Pharmacol. Toxicol*. 2001. **41**: 443–470.
doi.org/10.1146/annurev.pharmtox.41.1.443.

[70] Liao G. J., Clark A. S., Schubert E. K., Mankoff D. A. ^{18}F-Fluoroestradiol PET: Current Status and Potential Future Clinical Applications. *J. Nucl. Med*. 2016. **57**(8): 1269–1275.
doi.org/10.2967/jnumed.116.175596.

[71] Wiebe L. I. *PET radiopharmaceuticals for metabolic imaging in oncology*. In *International Congress Series*. Elsevier, 2004. 1264: 53–76.
doi.org/10.1016/j.ics.2003.12.102.

[72] Glasspool R. M., Evans T. R. Clinical imaging of cancer metastasis. *Eur. J. Cancer*. 2000. **36**(13): 1661–1670.
doi.org/10.1016/S0959-8049(00)00154-4.

[73] Varagnolo L., Stokkel M. P., Mazzi U., Pauwels E. K. ^{18}F-labeled radiopharmaceuticals for PET in oncology, excluding FDG. *Nucl. Med. Biol*. 2000. **27**(2): 103–112.
doi.org/10.1016/S0969-8051(99)00109-2.

[74] Adam M. J., Wilbur D. S. Radiohalogens for imaging and therapy. *Chem. Soc. Rev*. 2005. **34**(2): 153–163.
doi.org/10.1039/B313872K.

[75] Peterson L. M., Mankoff D. A., Lawton T. *et al*. Quantitative imaging of estrogen receptor expression in breast cancer with PET and

18F-fluoroestradiol. *J. Nucl. Med*. 2008. **49**(3): 367–374. doi.org/10.2967/jnumed.107.047506.

[76] Paquette M., Lavallée É., Phoenix S. *et al*. Improved estrogen receptor assessment by PET using the novel radiotracer 18F-4FMFES in estrogen receptor–positive breast cancer patients: an ongoing phase II clinical trial. *J. Nucl. Med*. 2018. **59**(2): 197–203. doi.org/10.2967/jnumed.117.194654.

[77] Chae S. Y., Ahn S. H., Kim S. B. *et al*. Diagnostic accuracy and safety of 16α-[^{18}F] fluoro-17β-oestradiol PET-CT for the assessment of oestrogen receptor status in recurrent or metastatic lesions in patients with breast cancer: a prospective cohort study. *Lancet Oncol*. 2019. **20**(4): 546–555. doi: 10.1016/S1470-2045(18)30936-7.

[XX] Peterson L. M., Kurland B. F., Schubert E. K. *et al*. A Phase 2 Study of 16α-[^{18}F]-fluoro-17β-estradiol Positron Emission Tomography (FES-PET) as a Marker of Hormone Sensitivity in Metastatic Breast Cancer (MBC). *Mol. Imaging Biol*. 2014. **16**(3): 431–440. doi.org/10.1007/s11307-013-0699-7.

[78] Kiesewetter D. O., Kilbourn M. R., Landvatter S. W. *et al*. Preparation of four fluorine-18-labeled estrogens and their selective uptakes in target tissues of immature rats. *J. Nucl. Med*. 1984. **25**(11): 1212–1221.

[79] Kumar P., Mercer J., Doerkson C. *et al*. Clinical production, stability studies and PET imaging with 16-alpha-[18F]fluoroestradiol ([18F] FES) in ER positive breast cancer patients. *J. Pharm. Pharm. Sci*. 2007. **10**(2): 256s–265s.

[80] Lim J. L., Zheng L., Berridge M. S., Tewson T. J. The use of 3-methoxymethyl-16β, 17β-epiestriol-*O*-cyclic sulfone as the precursor in the synthesis of F-18 16α-fluoroestradiol. *Nucl. Med. Biol*. 1996. **23**(7): 911–915. doi.org/10.1016/S0969-8051(96)00126-6.

[81] Dixit M., Shi J., Wei L. *et al*. Synthesis of Clinical-Grade [^{18}F]-Fluoroestradiol as a Surrogate PET Biomarker for the Evaluation of Estrogen Receptor-Targeting Therapeutic Drug. *Int. J. Mol. Imaging*. 2013. **2013**: 278607. doi.org/10.1155/2013/278607.

[82] Jabbour E., Issa J. P., Garcia-Manero G., Kantarjian H. Evolution of decitabine development: accomplishments, ongoing investigations, and future strategies. *Cancer: Interdis. Int. J. Am. Cancer Soc*. 2008. **112**(11): 2341–2351. doi.org/10.1002/cncr.23463.

[83] Ueda K., Masuda A., Fukuda M. *et al*. Monophosphorylation by deoxycytidine kinase affects apparent cellular uptake of decitabine in HCT116 colon cancer cells. *Drug Metab. Pharmacok*. 2017. **32**(6): 301–310. doi.org/10.1016/j.dmpk.2017.10.001.

[84] Duchmann M., Itzykson R. Clinical update on hypomethylating agents. *Int. J. Hematol*. 2019. **110**(2): 161–169. doi.org/10.1007/s12185-019-02651-9.

[85] Belyakov S., Hamilton G. S., Duvall B. *et al*. AU2016213880B2, 2016.

[86] Camiener G. W. Studies of the enzymatic deamination of cytosine arabinoside—III: Substrate requirements and inhibitors of the deaminase of human liver. *Biochem. Pharmacol*. 1967. **16**(9): 1691–1702. doi.org/10.1016/0006-2952(67)90244-4.

[87] Hosono H., Kuno S. The purification and properties of cytidine deaminase from *Escherichia coli*. *J. Biochem*. 1973. **74**(4): 797–803. doi.org/10.1093/oxfordjournals.jbchem.a130305.

[88] Teh A. H., Kimura M., Yamamoto M. *et al*. The 1.48 Å resolution crystal structure of the homotetrameric cytidine deaminase from mouse. *Biochemistry*. 2006. **45**(25): 7825–7833. doi.org/10.1021/bi060345f.

[89] Costanzi S., Vilar S., Micozzi D. *et al*. Delineation of the molecular mechanisms of nucleoside recognition by cytidine deaminase through virtual screening. *ChemMedChem*. 2011. **6**(8): 1452–1458. doi.org/10.1002/cmdc.201100139.

[90] Ferraris D., Duvall B., Delahanty G. *et al*. Design, synthesis, and pharmacological evaluation of fluorinated tetrahydrouridine

derivatives as inhibitors of cytidine deaminase. *J. Med. Chem*. 2014. **57**(6): 2582–2588. doi.org/10.1021/jm401856k.

[91] Oganesian A., Redkar S., Taverna P. Preclinical data in cynomolgus (cyn) monkeys of ASTX727, a novel oral hypomethylating agent (HMA) composed of low-dose oral decitabine combined with a novel cytidine deaminase inhibitor (CDAi). *Blood*. 2013. **122**(21): 2526. doi.org/10.1182/blood.V122.21.2526.2526.

[92] Savona M. R., Odenike O., Amrein P. C. *et al.* An oral fixed-dose combination of decitabine and cedazuridine in myelodysplastic syndromes: a multicentre, open-label, dose-escalation, phase 1 study. *Lancet Haematol*. 2019. **6**(4): e194–e203. doi: 10.1016/S2352-3026(19)30030-4.

[93] Garcia-Manero G., Griffiths E. A., Steensma D. P. *et al.* Oral cedazuridine/decitabine for MDS and CMML: a phase 2 pharmacokinetic/pharmacodynamic randomized crossover study. *Blood*. 2020. **136**(6): 674–683. doi.org/10.1182/blood.2019004143.

[94] Dhillon S. Decitabine/cedazuridine: first approval. *Drugs*. 2020. **80**(13): 1373–1378. doi.org/10.1007/s40265-020-01389-7.

[95] Norton J., Matsuo H., Sturla S. J. Synthesis of deoxytetrahydrouridine. *J. Org. Chem*. 2009. **74**(5): 2221–2223. doi.org/10.1021/jo802599v.

[96] Deeks E. D. Belzutifan: first approval. *Drugs*. 2021. **81**(16): 1921–1927. doi.org/10.1007/s40265-021-01606-x.

[97] Choueiri T. K., Bauer T. M., Papadopoulos K. P. *et al.* Inhibition of hypoxia-inducible factor-2α in renal cell carcinoma with belzutifan: a phase 1 trial and biomarker analysis. *Nat. Med*. 2021. **27**(5): 802–805. doi.org/10.1038/s41591-021-01324-7.

[98] Jaakkola P., Mole D. R., Tian Y.-M. *et al.* Targeting of HIF-α to the von Hippel-Lindau Ubiquitylation Complex by O_2-Regulated Prolyl Hydroxylation. *Science*. 2001. **292**(5516): 468–472. doi: 10.1126/science.105979.

[99] Bruick R. K., McKnight S. L. A Conserved Family of Prolyl-4-Hydroxylases That Modify HIF. *Science*. 2001. **294**(5545): 1337–1340. doi: 10.1126/science.1066373.

[100] Scheuermann T. H., Tomchick D. R., Machius M. *et al.* Artificial ligand binding within the HIF2α PAS-B domain of the HIF2 transcription factor. *Proc. Natl. Acad. Sci U. S. A*. 2009. **106**(2): 450–455. doi.org/10.1073/pnas.0808092106.

[101] Scheuermann T. H., Li Q., Ma H. W. *et al.* Allosteric inhibition of hypoxia inducible factor-2 with small molecules. *Nat. Chem. Biol*. 2013. **9**(4): 271–276. doi.org/10.1038/nchembio.1185.

[102] Rogers J. L., Bayeh L., Scheuermann T. H., *et al.* Development of Inhibitors of the PAS-B Domain of the HIF-2α Transcription Factor. *J. Med. Chem*. 2013. **56**(4): 1739–1747. doi.org/10.1021/jm301847z.

[103] Scheuermann T. H., Stroud D., Sleet C. E. *et al.* Isoform-Selective and Stereoselective Inhibition of Hypoxia Inducible Factor-2. *J. Med. Chem*. 2015. **58**(15): 5930–5941. doi.org/10.1021/acs.jmedchem.5b00529.

[104] Wehn P. M., Rizzi J. P., Dixon D. D. *et al.* Design and Activity of SpecificHypoxia-Inducible Factor-2α (HIF-2α) Inhibitors for the Treatment of Clear CellRenalCell-Carcinoma: Discovery of Clinical Candidate (*S*)-3-((2,2-Difluoro-1-hydroxy-7-(methylsulfonyl)-2,3-dihydro-1*H*-inden-4-yl)oxy)-5-fluorobenzonitrile (PT2385). *J. Med. Chem*. 2018. **61**(21): 9691–9721. doi.org/10.1021/acs.jmedchem.8b01196.

[105] Wallace E. M., Rizzi J. P., Han G. *et al.* A small-molecule antagonist of HIF2α is efficacious in preclinical models of renal cell carcinoma. *Cancer Res*. 2016. **76**(18): 5491–5500. doi.org/10.1158/0008-5472.CAN-16-0473.

[106] Cho H., Du X., Rizzi J. P. *et al.* On-target efficacy of a HIF-2α antagonist in preclinical kidney cancer models. *Nature*. 2016. **539**(7627): 107–111.

doi.org/10.1038/nature19795.
[107] Chen W., Hill H., Christie A. *et al*. Targeting renal cell carcinoma with a HIF-2 antagonist. *Nature*. 2016. **539**(7627): 112–117. doi.org/10.1038/nature19796.
[108] Xu R., Wang K., Rizzi J. P. *et al*. 3-[(1*S*,2*S*,3*R*)-2,3-Difluoro-1-hydroxy-7-methylsulfonylindan-4-yl] oxy-5-fluorobenzonitrile (PT2977), a Hypoxia-Inducible Factor 2α (HIF-2α) Inhibitor for the Treatment of Clear Cell Renal Cell Carcinoma. *J. Med. Chem*. 2019. **62**(15): 6876–6893. doi.org/10.1021/acs.jmedchem.9b00719.
[109] Choueiri T. K., Motzer R. J. Systemic therapy for metastatic renal-cell carcinoma. *New Eng. J. Med*. 2017. **376**(4): 354–366. doi: 10.1056/NEJMra1601333.
[110] Josey J. A., Shrimali R., Wallace E. M., Wong T. WO 2019191227, 2019.
[111] Louis D. N., Perry A., Wesseling P. *et al.*The 2021 WHO classification of tumors of the central nervous system: a summary. *Neuro-oncology*. 2021. **23**(8): 1231–1251. doi.org/10.1093/neuonc/noab106.
[112] Schaff L. R., Mellinghoff I. K. Glioblastoma and other primary brain malignancies in adults: a review. *JAMA*. 2023. **329**(7): 574–587. doi:10.1001/jama.2023.0023.
[113] Parsons D. W., Jones S., Zhang X. *et al*. An integrated genomic analysis of human glioblastoma multiforme. *Science*. 2008. **321**(5897): 1807–1812. doi: 10.1126/science.1164382.
[114] Yan H., Parsons D. W., Jin G. *et al*. IDH1 and IDH2 mutations in gliomas. *New Eng. J. Med*. 2009. **360**(8): 765–773. doi: 10.1056/NEJMoa0808710.
[115] Hartmann C., Meyer J., Balss J. *et al*. Type and frequency of IDH1 and IDH2 mutations are related to astrocytic and oligodendroglial differentiation and age: a study of 1,010 diffuse gliomas. *Acta Neuropathol*. 2009. **118**: 469–474. doi.org/10.1007/s00401-009-0561-9.
[116] Solomou G., Finch A., Asghar A. *et al*. Mutant IDH in gliomas: Role in cancer and treatment options. *Cancers*. 2023. **15**(11): 2883. doi.org/10.3390/cancers15112883.
[117] Lu C., Ward P. S., Kapoor G. S. *et al*. IDH mutation impairs histone demethylation and results in a block to cell differentiation. *Nature*. 2012. **483**(7390): 474–478. doi.org/10.1038/nature10860.
[118] Xu W., Yang H., Liu Y. *et al*. Oncometabolite 2-hydroxyglutarate is a competitive inhibitor of α-ketoglutarate-dependent dioxygenases. *Cancer Cell*. 2011. **19**(1): 17–30. doi: 10.1016/j.ccr.2010.12.014.
[119] Cancer Genome Atlas Research Network, Brat D. J., Verhaak R. G., Aldape K. D. *et al*. Comprehensive, Integrative Genomic Analysis of Diffuse Lower-Grade Gliomas. *New Engl. J. Med*. 2015. **372**(26): 2481–2498. doi: 10.1056/NEJMoa1402121.
[120] Eckel-Passow J. E., Lachance D. H., Molinaro A. M. *et al*. Glioma Groups Based on 1p/19q, IDH, and TERT Promoter Mutations in Tumors. *New Eng. J. Med*. 2015. **372**(26): 2499–2508. doi: 10.1056/NEJMoa1407279.
[121] Mandonnet E., Delattre J. Y., Tanguy M. L. *et al*. Continuous growth of mean tumor diameter in a subset of grade II gliomas. *Ann. Neurol*. 2003. **53**(4): 524–528. doi.org/10.1002/ana.10528.
[122] Rees J., Watt H., Jäger H. R. *et al*. Volumes and growth rates of untreated adult low-grade gliomas indicate risk of early malignant transformation. *Eur. J. Radiol*. 2009. **72**(1): 54–64. doi.org/10.1016/j.ejrad.2008.06.013.
[123] Lamb Y. N. Vorasidenib: First Approval. *Drugs*. 2024. **84**(10): 1325–1331. doi.org/10.1007/s40265-024-02097-2.
[124] Liu S., Abboud M., Mikhailov V. *et al*. Differentiating Inhibition Selectivity and Binding Affinity of Isocitrate Dehydrogenase 1 Variant Inhibitors. *J. Med. Chem*. 2023. **66**(7): 5279–5288.

doi.org/10.1021/acs.jmedchem.3c00203.
[125] Popovici-Muller J., Lemieux R. M., Artin E. *et al.* Discovery of AG-120 (Ivosidenib): A First-in-Class Mutant IDH1 Inhibitor for the Treatment of IDH1 Mutant Cancers. *ACS Med. Chem. Lett*. 2018. **9**(4): 300–305. doi.org/10.1021/acsmedchemlett.7b00421.
[126] Yen K., Travins J., Wang F. *et al.* AG-221, a first-in-class therapy targeting acute myeloid leukemia harboring oncogenic IDH2 mutations. *Cancer Discov*. 2017. **7**(5): 478–493. doi.org/10.1158/2159-8290.CD-16-1034.
[127] Mellinghoff I. K., Van Den Bent M. J., Blumenthal D. T. *et al.* Vorasidenib in IDH1-or IDH2-Mutant Low-Grade Gglioma. *New Eng. J. Med*. 2023. **389**(7): 589–601. doi: 10.1056/NEJMoa2304194.
[128] Dang L., White D. W., Gross S. *et al.* Cancer-associated IDH1 mutations produce 2-hydroxyglutarate. *Nature*. 2009. **462**(7274): 739–744. doi.org/10.1038/nature08617.
[129] Ward P. S., Patel J., Wise D. R. *et al.* The common feature of leukemia-associated IDH1 and IDH2 mutations is a neomorphic enzyme activity converting α-ketoglutarate to 2-hydroxyglutarate. *Cancer Cell*. 2010. **17**(3): 225–234. doi: 10.1016/j.ccr.2010.01.020.
[130] Mellinghoff I. K., Penas-Prado M., Peters K. B. *et al.* Vorasidenib, a dual inhibitor of mutant IDH1/2, in recurrent or progressive glioma; results of a first-in-human phase I trial. *Clin. Cancer Res*. 2021. **27**(16): 4491–4499. doi.org/10.1158/1078-0432.CCR-21-0611.
[131] Rudà R., Horbinski C., van den Bent M. *et al.* IDH inhibition in gliomas: from preclinicalmodels to clinical trials. *Nat. Rev. Neurol*. 2024. **20**(7): 395–407. doi: 10.1038/s41582-024-00967-7.
[132] Bombino A., Magnani M., Conti A. A Promising Breakthrough: The Potential of VORASIDENIB in the Treatment of Low-grade Glioma. *Curr. Mol. Pharmacol.* 2024. **17**(1): e18761429290327. doi.org/10.2174/0118761429290327240222061812.
[133] Konteatis Z. D., Popovici-Muller J., Travins J. M. *et al.* PT WO 2015003640 A1, 2015.
[134] Moore J. L., Taylor S. M., Soloshonok V. A. An efficient and operationally convenient general synthesis of tertiary amines by direct alkylation of secondary amines with alkyl halides in the presence of Huenig's base. *Arkivoc*. 2005. **2005**(vi): 287–292. doi.org/10.3998/ark.5550190.0006.624.
[135] Soloshonok V. A., Ono T. The effect of substituents on the feasibility of azomethine-azomethine isomerization: new synthetic opportunities for biomimetic transamination. *Tetrahedron*. 1996. **52**(47): 14701–14712. doi.org/10.1016/0040-4020(96)00920-9.
[136] Ohkura H., Berbasov D. O., Soloshonok V. A. Chemo-and regioselectivity in the reactions between highly electrophilic fluorine containing dicarbonyl compounds and amines. Improved synthesis of the corresponding imines/enamines. *Tetrahedron*. 2003. **59**(10): 1647–1656. doi.org/10.1016/S0040-4020(03)00138-8.
[137] Soloshonok V. A., Kirilenko A. G., Kukhar V. P., Resnati G. Transamination of fluorinated β-keto carboxylic esters. A biomimetic approach to β-polyfluoroalkyl-β-amino acids. *Tetrahedron Lett*. 1993. **34**(22): 3621–3624. doi.org/10.1016/S0040-4039(00)73652-5.
[138] Soloshonok V. A., Kirilenko A. G., Fokina N. A. *et al.* Chemo-enzymatic approach to the synthesis of each of the four isomers of α-alkyl-β-fluoroalkyl-substituted β-amino acids. *Tetrahedron: Asymmetry*. 1994. **5**(7): 1225–1228. doi.org/10.1016/0957-4166(94)80163-0.
[139] Soloshonok V. A., Kirilenko A. G., Galushko S. V., Kukhar V. P. Catalytic asymmetric synthesis of β-fluoroalkyl-β-amino acids via biomimetic [1,3]-proton shift reaction. *TetrahedronLett*. 1994. **35**(28): 5063–5064.

doi: 10.1016/S0040-4039(00)73320-X.
[140] Soloshonok V. A., Ono T., Soloshonok I. V. Enantioselective biomimetic transamination of β-keto carboxylic acid derivatives. An efficient asymmetric synthesis of β-fluoroalkyl β-amino acids. *J. Org.Chem*. 1997. **62**(22): 7538–7539.
doi: 10.1021/jo9710238.
[141] Soloshonok V. A., Kukhar V. P. Biomimetic transamination of α-keto perfluorocarboxylic esters. An efficient preparative synthesis of β,β,β-trifluoroalanine. *Tetrahedron*. 1997. **53**(25): 8307–8314.
doi: 10.1016/S0040-4020(97)00517-6.
[142] Hoy S. M. Oteseconazole: First Approval. *Drugs*. 2022. **82**: 1017–1023.
doi: 10.6084/m9.figshare.19896604.
[143] Warrilow A. G., Hull C. M., Parker J. E. *et al*. The clinical candidate VT-1161 is a highly potent inhibitor of Candida albicans CYP51 but fails to bind the human enzyme. *Antimicrob. Agents Chemother*. 2014. **58**(12): 7121–7127.
doi.org/10.1128/aac.03707-14.
[144] Garvey E. P., Hoekstra W. J., Moore W. R. *et al*. VT-1161 dosed once daily or once weekly exhibits potent efficacy in treatment of dermatophytosis in a guinea pig model. *Antimicrob. Agents Chemother*. 2015. **59**(4): 1992–1997.
doi.org/10.1128/aac.04902-14.
[145] Martens M. G., Maximos B., Degenhardt T. *et al*. Phase 3 study evaluating the safety and efficacy of oteseconazole in the treatment of recurrent vulvovaginal candidiasis and acute vulvovaginal candidiasis infections. *Am. J. Obstet. Gynecol*. 2022. **227**(6): 880-e1.
doi.org/10.1016/j.ajog.2022.07.023.
[146] Hoekstra W. J., Garvey E. P., Moore W. R. *et al*. Design and optimization of highly-selective fungal CYP51 inhibitors. *Bioorg. Med. Chem. Lett*. 2014. **24**(15): 3455–3458.
doi.org/10.1016/j.bmcl.2014.05.068.
[147] Hoekstra W. J., Yates C. M. Antifungal compound process. WO 2015143142 A1, 2015.
[148] Ali I., Alam S. D., Al-Othman Z. A., Farooqi J. A. Recent advances in SPE–chiral-HPLC methods for enantiomeric separation of chiral drugs in biological samples. *J. Chromatogr. Sci.* 2013. **51**(7): 645–654.
doi.org/10.1093/chromsci/bms262.
[149] Marek W. K., Lee J. W., Seidel-Morgenstern A., Antos D. Separation of nonracemic mixtures of enantiomers by achiral simulated moving bed chromatography. *Sep. Purif. Technol*. 2025. **361**(3): 131497.
doi.org/10.1016/j.seppur.2025.131497.
[150] Yasumoto M., Ueki H., Soloshonok V. A. Self-disproportionation of enantiomers of 3,3,3-trifluorolactic acid amides via sublimation. *J. Fluor. Chem*. 2010. **131**(2): 266–269.
doi.org/10.1016/j.jfluchem.2009.10.002.
[151] Han J., Wzorek A., Kwiatkowska M. *et al*. The self-disproportionation of enantiomers (SDE) of amino acids and their derivatives. *Amino Acids*. 2019. **51**(6): 865–889.
doi.org/10.1007/s00726-019-02729-y.
[152] Wzorek A., Klika K. D., Drabowicz J. *et al*. The self-disproportionation of the enantiomers (SDE) of methyl *n*-pentyl sulfoxide *via* achiral, gravity-driven column chromatography: a case study. *Org. Biomol. Chem*. 2014. **12**(26): 4738–4746.
doi: 10.1039/c4ob00831f.
[153] Segal-Maurer S., DeJesus E., Stellbrink H. J. *et al*. Capsid Inhibition with Lenacapavir in Multidrug-Resistant HIV-1 Infection. *New Eng. J. Med.* 2022. **386**(19): 1793–1803.
doi: 10.1056/NEJ Moa2115542.
[154] Thenin-Houssier S., Valente S. HIV-1 capsid inhibitors as antiretroviral agents. *Curr. HIV Res*. 2016. **14**(3): 270–282.
doi: 10.2174/1570162x14999160224103555.
[155] Carnes S. K., Sheehan J. H., Aiken C. Inhibitors of the HIV-1 capsid, a target of opportunity. *Curr. Opin. HIV AIDS*. 2018. **13**(4): 359–365.
doi: 10.1097/COH.0000000000000472.
[156] Scott D. E., Bayly A. R., Abell C., Skidmore J. Small molecules, big targets: drug discovery

faces the protein–protein interaction challenge. *Nat. Rev. Drug Discov*. 2016. **15**(8): 533–550. doi.org/10.1038/nrd.2016.29.

[157] Freed E. O. HIV-1 assembly, release and maturation. *Nat. Rev. Microbiol*. 2015. **13**(8): 484–496. doi.org/10.1038/nrmicro3490.

[158] Ganser B. K., Li S., Klishko V. Y. *et al*. Assembly and analysis of conical models for the HIV-1 core. *Science*. 1999. **283**(5398): 80–83. doi: 10.1126/science.283.5398.

[159] Yamashita M., Engelman A. N. Capsid-dependent host factors in HIV-1 infection. *Trends Microbiol*. 2017. **25**(9): 741–755. doi: 10.1016/j.tim.2017.04.004.

[160] Huang P. T., Sum mers B. J., Xu C. *et al*. FEZ1 is recruited to a conserved cofactor site on capsid to promote HIV-1 trafficking. *Cell Rep*. 2019. **28**(9): 2373–2385. doi: 10.1016/j.celrep.2019.07.079.

[161] Fernandez J., Machado A. K., Lyonnais S. *et al*. Transportin-1 binds to the HIV-1 capsid via a nuclear localization signal and triggers uncoating. *Nat. Microbiol*. 2019. **4**(11): 1840–1850. doi.org/10.1038/s41564-019-0575-6.

[162] US Food and Drug Administration. FDA approves new HIV drug for adults with limited treatment options. 2023.

[163] Zhou L., Sokolskaja E., Jolly C. *et al*. Transportin 3 promotes a nuclear maturation step required for efficient HIV-1 integration. *PLoS Pathog*. 2011. **7**(8): e1002194. doi.org/10.1371/journal.ppat.1002194.

[164] Link J. O., Rhee M. S., Tse W. C. *et al*. Clinical targeting of HIV capsid protein with a long-acting small molecule. *Nature*. 2020. **584**(7822): 614–618. doi.org/10.1038/s41586-020-2443-1.

[165] Bester S. M., Wei G., Zhao H. *et al*. Structural and mechanistic bases for a potent HIV-1 capsid inhibitor. *Science*. 2020. **370**(6514): 360–364. doi: 10.1126/science.abb4808.

[166] Singh K., Gallazzi F., Hill K. J. GS-CA Compounds: First-In-Class HIV-1 Capsid Inhibitors Covering Multiple Grounds. *Front. Microbiol*. 2019. **10**: 1227. doi.org/10.3389/fmicb.2019.01227.

[167] Margot N., Ram R., Rhee M., Callebaut C. Absence of lenacapavir (GS-6207) phenotypic resistance in HIV gag cleavage site mutants and in isolates with resistance to existing drug classes. *Antimicrob. Agents Chemother*. 2021. **65**(3): 10–128. doi.org/10.1128/aac.02057-20.

[168] Bekerman E., Blari W. S., Chiu A. *et al*. Capsid inhibitors for prevention of HIV. US2021188815A1, 2021.

[169] Ellman J. A. Applications of tert-butanesulfinamide in the asymmetric synthesis of amines. *Pure App. Chem*. 2003. **75**(1): 39–46. doi.org/10.1351/pac200375010039.

[170] Robak M. T., Herbage M. A., Ellman J. A. Synthesis and Applications of *tert*-Butanesulfinamide. *Chem. Rev*. 2010. **110**(6): 3600–3740. doi.org/10.1021/cr900382t.

[171] Xie C., Wu L., Mei H. *et al*. Generalized access to fluorinated β-keto amino compounds through asymmetric additions of α,α-difluoroenolates to CF_3-sulfinylimine. *Org. Biomol. Chem*. 2014. **12**(39): 7836–7843. doi: 10.1039/C4OB01575D.

[172] Xie C., Dai, Y., Mei H. *et al*. Asymmetric synthesis of quaternary α-fluoro-β-keto-amines *via*detrifluoroacetylative Mannich reactions. *Chem. Commun*. 2015. **51**(44): 9149–9152. doi: 10.1039/c5cc02256h.

[173] Drug Trials Snapshots: VOYDEYA. Available at https://www.fda.gov/drugs/drug-approvals-and-databases/drug-trials-snapshots-voydeya.

[174] Hao J., Milcent T., Retailleau P. *et al*. Asymmetric Synthesis of Cyclic Fluorinated Amino Acids. *Eur. J. Org. Chem*. 2018. **2018**(27–28): 3688–3692. doi: 10.1002/ejoc.201800255.

[175] Sato T., Izaw K., Aceña J. L. *et al*. Tai-

lor-Madeα-Amino Acids in thePharmaceuticalIndustry: SyntheticApproachesto (1*R*,2*S*)-1-Amino-2-vinylcyclopropane-1-carboxylic A cid (Vinyl-ACCA). *Eur. J. Org. Chem*. 2016. **2016**(16): 2757–2774. doi: 10.1002/ejoc.201600112.

[176] Cai C., Soloshonok V. A., Hruby V. J. Michael Addition Reactions Between Chiral Ni(II) Complex of Glycine and 3-(*trans*-Enoyl)oxazolidin-2-ones. A Case of Electron Donor–Acceptor Attractive Interaction-Controlled Face Diastereoselectivity. *J. Org. Chem*. 2001. **66**(4): 1339–1350. doi: 10.1021/jo0014865.

[177] Soloshonok V. A., Ueki H., Tiwari R. *et al*. Virtually Complete Control of Simple and Face Diastereoselectivity in the Michael Addition Reactions between Achiral Equivalents of a Nucleophilic Glycine and (*S*)- or (*R*)-3-(*E*-Enoyl)-4-phenyl-1,3-oxazolidin-2-ones: Practical Method for Preparation of β-Substituted Pyroglutamic Acids and Prolines. *J. Org. Chem*. 2004. **69**(15): 4984–4990. doi: 10.1021/jo0495438.

[178] Soloshonok V. A., Ueki H., Ellis T. K. *et al*. Application of modular nucleophilic glycine equivalents for truly practical asymmetric synthesis of β-substituted pyroglutamic acids. *Tetrahedron Lett*. 2005. **46**(7): 1107–1110. doi: 10.1016/j.tetlet.2004.12.093.

[179] Wiles J. A., Phadke A. S., Deshpande M. *et al*. Achillion Pharmaceuticals Inc. Aryl, heteroaryl, and heterocyclic compounds for treatment of medical disorders. U.S. Patent Application 2018305375 A1, 2018.

[180] Wiles J. A., Phadke A. S., Deshpande M., Agarwal A., Chen D., Gadhachanda V. R., Hashimoto A., Pais G., Wang Q., Wang X. Achillion Pharmaceuticals Inc. Aryl, heteroaryl, and heterocyclic compounds for treatment of medical disorders. U.S. Patent 10822352 B2, 2020.

[181] Kang C. Danicopan: First Approval. *Drugs*. 2024. **84**(5): 613–618. doi:10.1007/s40265-024-02023-6.

[182] Verdin P. FDA new drug approvals in Q1 2024. *Nat. Rev. Drug Discov*. 2024. **23**(5): 331. doi:10.1038/d41573-024-00063-x.

[183] Kulasekararaj A. G., Lazana I. Paroxysmal nocturnal hemoglobinuria: Where are we going. *Am. J. Hematol*. 2023. **98**(S5): S33–S43. doi:10.1002/ajh.26882.

[184] Voydeya (Danicopan) granted first-ever regulatory approval in Japan for adults with PNH to be used in combination with C5 inhibitor therapy. Available at https://www.astrazeneca.com./media-centre/press-releases/2024/voydeya-danicopan-granted-first-ever-regulatory-approval-in-japan-for-adults-with-pnh-to-be-used-in-combination-with-c5-inhibitor-therapy.html.

[185] First oral treatment against residual haemolytic anaemia in patients with paroxysmal nocturnal haemoglobinuria. Available at https://www.ema.europa.eu/en/news/first-oral-treatment-against-residual-haemolytic-anaemia-patients-paroxysmal-nocturnal-haemoglobinuria.

[186] Wiles J. A., Phadke A. S., Deshpande M. *et al*. Achillion Pharmaceuticals Inc. Aryl, heteroaryl, and heterocyclic compounds for treatment of medical disorders. WO 2017035353A1, 2017.

[187] Phadke A., Hashimoto A., Andres M., Achillion Pharmaceuticals Inc. Morphic forms of complement factor D inhibitors. WO 2020069024A1, 2020.

[188] Phadke A. Achillion Pharmaceuticals Inc. Morphic forms of complement factor D inhibitors. WO 2020051538A1, 2020.

[189] Aslan B., Kismali G., Iles L. R. *et al*. Pirtobrutinib inhibits wild-type and mutant Bruton's tyrosine kinase-mediated signaling in chronic lymphocytic leukemia. *BloodCancer J*. 2022. **12**(5): 80. doi.org/10.1038/s41408-022-00675-9.

[190] Gomez E. B., Ebata K., Randeria H. S. *et al.*

Preclinical characterization of pirtobrutinib, a highly selective, noncovalent (reversible) BTK inhibitor. *Blood*. 2023. **142**(1): 62–72. doi.org/10.1182/blood.2022018674.

[191] Thompson P. A., Tam C. S. Pirtobrutinib: a new hope for patients with BTK inhibitor–refractory lymphoproliferative disorders. *Blood*. 2023. **141**(26): 3137–3142. doi.org/10.1182/blood.2023020240.

[192] Telaraja D., Kasamon Y. L., Collazo J. S. *et al*. FDA approval summary: pirtobrutinib for relapsed or refractory mantle cell lymphoma. *Clin. Cancer Res*. 2024. **30**(1): 17–22. doi.org/10.1158/1078-0432.CCR-23-1272.

[193] Keam S. J. Pirtobrutinib: First Aapproval. *Drugs*. 2023. **83**(6): 547–553. doi.org/10.1007/s40265-023-01860-1.

[194] Arguelles D., Alonso J., Eary C. T. *et al*. PT WO 2022056100 A1, 2022.

[195] Guisot N. PT US 2021093611 A1, 2021.

[196] Turner N. C., Im S.-A., Saura C. *et al*. Inavolisib-based therapy in PIK3CA-mutated advanced breast cancer. *New Engl. J. Med*. 2024. **391**(17): 1584–1596. doi: 10.1056/NEJMoa2404625.

[197] Bartsch R. Next generation of drugs in breast cancer. *memo – Mag. Eur. Med. Oncol*. 2024. **17**(4): 280–286. doi: 10.1007/s12254-024-00999-1.

[198] Singh S., Bradford D., Li X. *et al*. FDA approval summary: Alpelisib for PIK3CA-related overgrowth spectrum. *Clin. Cancer Res*. 2024. **30**(1): 23–28. doi: 10.1158/1078-0432.CCR-23-1270.

[199] Sirico M., D'Angelo A., Gianni C. *et al*. Current State and Future Challenges for PI3K Inhibitors in Cancer Therapy. *Cancers*. 2023. **15**(3): 703. doi: 10.3390/cancers15030703.

[200] Salphati L., Pang J., Plise E. G. *et al*. Preclinical assessment of the PI3Kα selective inhibitor inavolisib and prediction of its pharmacokinetics and efficacious dose in human. *Xenobiotica*. 2024. **54**(10): 808–820. doi: 10.1080/00498254.2024.2415103.

[201] Shan K. S., Bonano-Rios A., Theik N. W. Y. *et al*. Molecular targeting of the phosphoinositide-3-protein kinase (PI3K) pathway across various cancers. *Int. J. Mol. Sci*. 2024. **25**(4): 1973. doi: 10.3390/ijms25041973.

[202] Belli C., Repetto M., Anand S. *et al*. The emerging role of PI3K inhibitors for solid tumour treatment and beyond. *Br. J. Cancer*. 2023. **128**(12): 2150–2162. doi: 10.1038/s41416-023-02221-1.

[203] Yu M., Chen J., Xu Z. *et al*. Development and safety of PI3K inhibitors in cancer. *Arch. Toxicol*. 2023. **97**(3): 635–650. doi: 10.1007/s00204-023-03440-4.

[204] Vanhaesebroeck B., Perry M. W. D., Brown J. R. *et al*. PI3K inhibitors are finally coming of age. *Nat. Rev. Drug Discov*. 2021. **20**(10): 741–769. doi: 10.1038/s41573-021-00209-1.

[205] Song K. W., Edgar K. A., Hanan E. J. *et al*. RTK-dependent inducible degradation of mutant PI3Kα drives GDC-0077 (Inavolisib) efficacy. *Cancer Discov*. 2022. **12**(1): 204–219. doi: 10.1158/2159-8290.CD-21-0072.

[206] Hanan E. J., Braun M.-G., Heald R. A. *et al*. Discovery of GDC-0077 (Inavolisib), a Highly Selective Inhibitor and Degrader of Mutant PI3Kα. *J. Med. Chem*. 2022. **65**(24): 16589–16621. doi: 10.1021/acs.jmedchem.2c01422.

[207] Lovering F., Bikker J., Humblet C. Escape from Flatland: Increasing Saturation as an Approach to Improving Clinical Success. *J. Med. Chem*. 2009. **52**(21): 6752–6756. doi.org/10.1021/jm901241e.

Стаття надійшла 27.01.2025.